



# Nanoceria: an innovative strategy for cancer treatment

Joyce L. Y. Tang<sup>1,2</sup> · Shehzahdi S. Moonshi<sup>1</sup> · Hang T. Ta<sup>1,2,3</sup>

Received: 17 June 2022 / Revised: 19 December 2022 / Accepted: 9 January 2023 / Published online: 19 January 2023  
© The Author(s) 2023, corrected publication 2023

## Abstract

Nanoceria or cerium oxide nanoparticles characterised by the co-existing of  $Ce^{3+}$  and  $Ce^{4+}$  that allows self-regenerative, redox-responsive dual-catalytic activities, have attracted interest as an innovative approach to treating cancer. Depending on surface characteristics and immediate environment, nanoceria exerts either anti- or pro-oxidative effects which regulate reactive oxygen species (ROS) levels in biological systems. Nanoceria mimics ROS-related enzymes that protect normal cells at physiological pH from oxidative stress and induce ROS production in the slightly acidic tumour microenvironment to trigger cancer cell death. Nanoceria as nanozymes also generates molecular oxygen that relieves tumour hypoxia, leading to tumour cell sensitisation to improve therapeutic outcomes of photodynamic (PDT), photothermal (PTT) and radiation (RT), targeted and chemotherapies. Nanoceria has been engineered as a nanocarrier to improve drug delivery or in combination with other drugs to produce synergistic anti-cancer effects. Despite reported preclinical successes, there are still knowledge gaps arising from the inadequate number of studies reporting findings based on physiologically relevant disease models that accurately represent the complexities of cancer. This review discusses the dual-catalytic activities of nanoceria responding to pH and oxygen tension gradient in tumour microenvironment, highlights the recent nanoceria-based platforms reported to be feasible direct and indirect anti-cancer agents with protective effects on healthy tissues, and finally addresses the challenges in clinical translation of nanoceria based therapeutics.

**Keywords** Nanomedicine · Cerium oxide · Redox-responsive nanozymes · Oxidative stress · Tumour hypoxia · Treatment development

## Introduction

Cancer is the general term utilised to demonstrate a heterogeneous group of diverse diseases characterised by rapid, uncontrolled growth of abnormal cells that can affect any part of the body. Cancer can metastasize and spread to other organs if not detected at an early stage, making it a difficult disease to treat, resulting in a leading cause of death globally [1]. The World Health Organisation's International Agency for Research (WHO IARC) <https://gco.iarc.fr/today/>

[online-analysis-pie](#) estimated 19.3 million cancer diagnosis with more than 50% mortality (9.96 million) in 2020. Despite advancements in cancer treatment strategies, cancers including lung, colorectal, prostate and stomach cancers still demonstrate poor five-year survival rate [2] especially with the COVID-19 global pandemic delaying diagnosis and disrupting access to cancer care and treatment options [3, 4]. Factors contributing to poor prognosis and cancer relapses including metastasis, intrinsic and acquired resistance to chemotherapeutic drugs revealed the ongoing need to enhance conventional therapies such as chemo- and radiation therapies, and to discover new, and innovative treatment approaches [5, 6]. One popular strategy is the engineering of redox-sensitive nanomaterials with the capability of regulating reactive oxygen species (ROS) in biological systems for desired treatment outcomes [7].

ROS including superoxide anions ( $O_2^-$ ), hydrogen peroxide ( $H_2O_2$ ), hydroxide radicals ( $\cdot OH$ ) and singlet oxygen ( $^1O_2$ ) are crucial for signal transduction and cell survival [8]. ROS levels in cells are tightly regulated by antioxidant

✉ Hang T. Ta  
h.ta@griffith.edu.au

<sup>1</sup> Queensland Micro- and Nanotechnology Centre, Griffith University, Nathan, QLD 4111, Australia

<sup>2</sup> Bioscience Discipline Department, School of Environment and Science, Griffith University, Nathan Campus, Brisbane, QLD 4111, Australia

<sup>3</sup> Australian Institute for Bioengineering and Nanotechnology, University of Queensland, St Lucia, QLD 4072, Australia

enzymes for redox homeostasis. Consequently, regulated ROS can promote both cell damage and cell survival and has been shown to be biologically important in autophagy, immune cell function, stem cell differentiation, cellular proliferation, and adaptation to hypoxia [9]. ROS was found to be associated with cancer, initially revealed by the elevated levels of ROS production in human tumour cells [10]. Further studies suggested that ROS have a dual role in cancer tumorigenesis and cancer cell survival via: (1) increased ROS production promoting pro-tumourigenic signalling events to facilitate cancer cell proliferation, metastasis, angiogenesis and adapting to hypoxia resulting in aggressive tumour growth; (2) reinforced ROS depletion to maintain ROS homeostasis below the toxic threshold [11]. Cancer cells adapting to tumour microenvironment (TME) have increased basal ROS level with a higher rate of both ROS production and ROS scavenging in comparison to healthy cells, which potentially increase their susceptibility to ROS or redox manipulation therapies [12]. Thus, enhancing ROS production and/or inhibiting ROS elimination to force excessive accumulation in tumours are feasible strategies as effective cancer therapies [7, 13, 14]. Several chemotherapeutics have been shown to increase ROS levels in cancer cells over the survival threshold and trigger oxidative stress-induced cancer cell death [13, 15]. Established anti-cancer drugs such as paclitaxel [16], doxorubicin [17] and cisplatin [18] promoted the accumulation of ROS beyond the tolerability threshold which contributed to their potent cytotoxicity effects. Cancer metastatic progression is a complex process consists of a series of sequential steps including cancer cells dissociation from a primary tumour, intravasation into and survival in the circulation, arrest in visceral organs, adhesion to endothelial cells, extravasation into tissues, proliferation and vascularisation of the metastatic lesions [19]. Throughout the metastatic progression, sublethal levels of ROS had been shown to be involved in activating/increasing the expression of various molecules closely related to the formation of metastatic colonies and angiogenesis including metalloproteinases, adhesion molecules, epidermal growth factor (EGF), EGF receptor and vascular endothelial growth factor (VEGF) [19]. Therefore, pro-oxidant therapeutic approaches that exacerbate oxidative stress on cancer cells could inhibit occurrence of distant metastasis not only through limiting cell survival, but also decreasing expression of pro-metastatic biomolecules that cancer cells interact with to promote metastatic progression [19, 20].

Nanoparticles (NPs) have been widely researched for use in medicine due to two key physicochemical properties: (1) high surface-to-volume ratios potentially increasing efficacy while decreasing biotoxicity; (2) high capabilities for multifunctionalisation especially through the incorporation of targeting ligands specific to disease types [21–23]. Nanomaterials can either exert cancer-killing effects themselves or

are fabricated as a hybrid nanosystem, comprising different functionalities such as nanocarrier, therapeutic and imaging agent to address the heterogeneity and complexity of TME [24, 25]. The use of NPs carrier can protect the therapeutic drug from chemical and enzymatic degradation and premature clearance, allowing sufficient drug dosage to reach tumour sites [26–28]. ROS-based NPs such as nanozymes, synthesised with intrinsic ROS generation and/or depletion properties can directly induce oxidative stress on tumour cells or sensitise cancerous tissues to induce desired therapeutic outcomes [29–31]. ROS-responsive nanoplatform also allows controlled and targeted delivery of drugs to tumour sites, whilst ensuring stability, plasma half-life and bioavailability of the drugs administered [32].

Cerium oxide NPs or nanoceria have then been taken into consideration as potential anti-cancer agent due to the unique chemistry of cerium oxide [33, 34]. Cerium is the most abundant element in the lanthanide series which is unique from other lanthanoid rare earth metals that exhibit in the trivalent state, as it can exist in two oxidation states: fully reduced trivalent cerous  $\text{Ce}^{3+}$  and fully oxidised tetravalent ceric  $\text{Ce}^{4+}$  [35, 36]. Cerous  $\text{Ce}^{3+}$  and ceric  $\text{Ce}^{4+}$  atoms co-exist on the lattice surface of nanoceria, presenting oxygen vacancies for reduction–oxidation reactions [35–37]. Cerium oxide NPs are utilised as nanozymes, mimicking the catalytic activity of redox enzymes such as superoxide dismutase (SOD), catalase, phosphatase, oxidase peroxidase, and phosphotriesterase, advantaging from their ability to rapidly convert between valency states [38]. The non-stoichiometry ratio of  $\text{Ce}^{3+}/\text{Ce}^{4+}$  on the surface determines the catalytic performance of the NPs and is shown to be affected by synthesis methods [38–40]. Cerium can easily alternate and adjust its electronic configuration responding to the immediate microenvironment. This ability allows nanoceria to manifest either antioxidant or pro-oxidant activities [33, 34, 41–43]. Its anti-oxidative effects have been employed in the development of numerous cerium oxide-based nanomaterials for ROS-related diseases [39, 42, 44, 45]. Studies in the anti-cancer potential of nanoceria emerged in recent years exploring its pro-oxidative effects inducing cancer cell death whilst the antioxidant properties suppressing tumour growth and protecting normal tissues from oxidative stress. Nanoceria has demonstrated significant therapeutic implications, either modulating ROS to kill or sensitise tumour cells while protecting neighbouring tissues or as a drug carrier to improve treatment outcomes and patient's prognosis (Fig. 1). A comprehensive review of the biomedical applications of nanoceria was published in 2021, covering a wide range of biological properties with a brief discussion on the anti-cancer activities of nanoceria [46]. Another review on a similar topic was published recently focusing on the use of nanoceria as biosensors in cancer diagnosis and as a chemical sensitiser for cancer therapies with limited

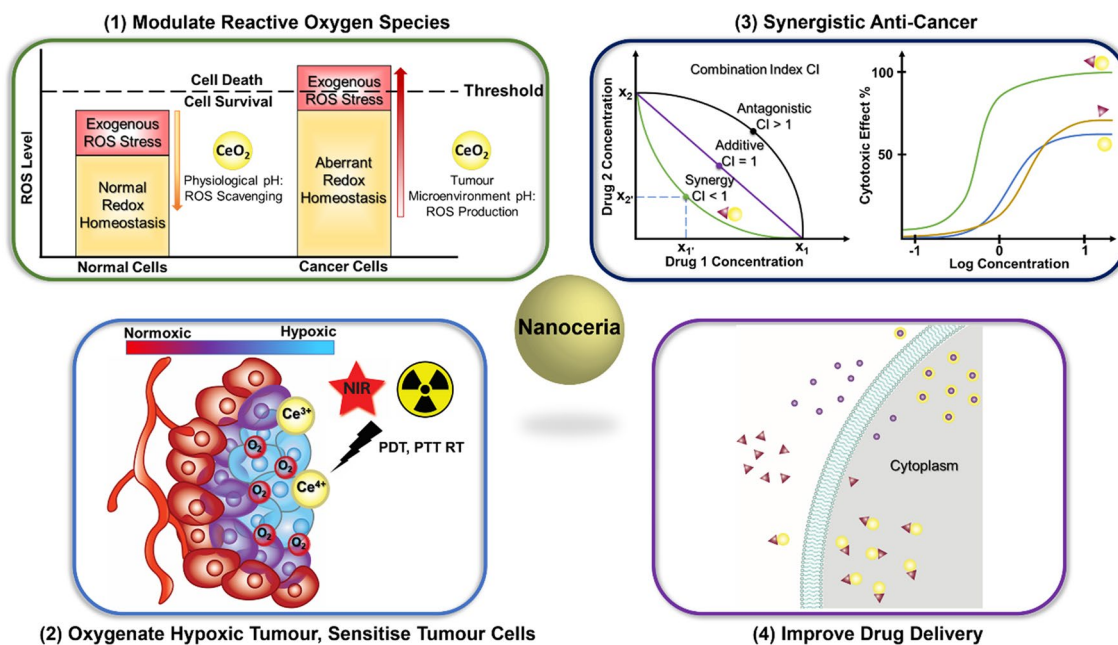


**Fig. 1** Applications of nanoceria in cancer treatment. (1) Protect normal cells from oxidative stress through ROS scavenging activities at physiological pH; induce oxidative stress on cancer cells through ROS production at slightly acidic tumour microenvironment. (2) Generate molecular oxygen to oxygenate hypoxic tumour and sensitise

tumour cells for photodynamic, photothermal and radiation therapies. (3) Enhance cancer killing through synergistic combination with other anti-cancer agents. (4) Act as nanocarriers to improve delivery of anti-cancer drugs

coverage on cancer-killing properties of nanoceria reported in the last 3 years [47]. The most recent summary of nanoceria's anti-cancer effects was a perspective article published in 2018 discussing the multifaceted activity of nanoceria in the prevention and treatment of cancer [48]. Therefore, our comprehensive review aims to summarise recent research on nanoceria in cancer treatment, focusing on the NPs' interventions in the adapted tumour redox environment.

## Dual-catalytic activities

The co-existing  $\text{Ce}^{3+}$  and  $\text{Ce}^{4+}$  on nanoceria make it self-sufficiently dual-catalytic, promoting both anti-oxidation and oxidation processes. The catalytic activities of nanoceria as nanozymes can be tuned at the synthesis steps, adjusting key physicochemical properties such as size, morphology, hetero-atom doping and surface modification [40, 49, 50]. The nanoceria crystals can be engineered to have different facet exposure and surface microstructures through varying synthesis conditions (amount of sodium hydroxide, reaction temperature, etc.) [51, 52]. This resulted in nanoceria of different morphologies and size: nanooctahedra (dominant [111] planes exposed), nanocubes (predominantly [100] surface facets) or nanorods ([100] and [111] or [110] planes exposed depending on synthetic procedures) [53], and that nanorods demonstrated highest peroxidase-like activity

due to having the most abundant defects and richest oxygen vacancies ( $\text{Ce}^{3+}$  dominating) detected on the surfaces [52]. This finding was further supported by Fu et al. where the authors reported the preparation of nanoceria with various morphologies using a one-step hydrothermal synthesis method. It was reported that rod shape nanoceria had a substantially higher percentage of  $\text{Ce}^{3+}$  (66.6%) over other morphology formulations (up to 26.8%) [54]. Doping with cations such as  $\text{Al}^{3+}$  impede the surface diffusion of Ce ions, forming  $-\text{Al}-\text{O}-\text{Ce}-\text{O}-$  clusters that significantly improved the reversible oxygen storage capacity of nanoceria [55]. Once applied in biological systems, the bioactive properties of nanoceria are generally determined from  $\text{Ce}^{3+}/\text{Ce}^{4+}$  ratio that are affected by the surrounding microenvironment, with pH and oxygen tensions being the pivotal factors (Fig. 2) [56].

## $\text{Ce}^{3+}/\text{Ce}^{4+}$

Nanoceria is characterised by the co-existence of fully oxidised  $\text{Ce}^{4+}$  and fully reduced  $\text{Ce}^{3+}$ . The  $\text{Ce}^{3+}/\text{Ce}^{4+}$  ratio presented on a surface lattice is instrumental in determining the catalytic properties of Ce. When  $\text{Ce}^{3+}$  is dominating, the NPs exhibit higher SOD-like activity that catalyses transformation of superoxide radicals to hydrogen peroxides and oxygen:  $\text{O}_2^- + \text{Ce}^{4+} \rightarrow \text{O}_2 + \text{Ce}^{3+}$  and  $\text{O}_2^- + \text{Ce}^{3+} + 2\text{H}^+ \rightarrow \text{H}_2\text{O}_2 + \text{Ce}^{4+}$  [57]. When  $\text{Ce}^{3+}/\text{Ce}^{4+}$  ratio is low, higher

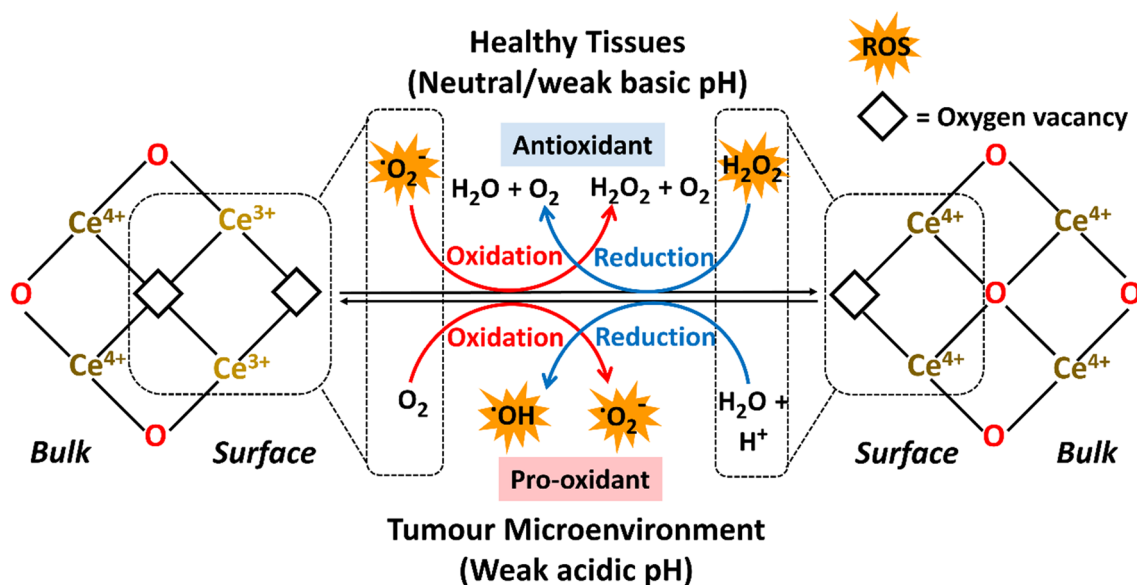


**Fig. 2** Nanoceria or cerium oxide nanoparticles are characterised as the co-existence of  $\text{Ce}^{3+}$  and  $\text{Ce}^{4+}$  with oxygen vacancies on the surface lattice. Depending on the immediate environment, nanoceria

exerts antioxidative activities at neutral pH that scavenges reactive oxygen species (ROS) within healthy tissues whilst acting as pro-oxidant producing ROS at the weak acidic tumour microenvironment

catalase- and phosphatase-mimetic activities catalysing the degradation of  $\text{H}_2\text{O}_2$  and phosphoric acid monoesters, respectively, are observed eg.  $\text{H}_2\text{O}_2 + 2\text{Ce}^{4+} \rightarrow 2\text{H}^+ + \text{O}_2 + 2\text{Ce}^{3+}$  and  $\text{H}_2\text{O}_2 + 2\text{Ce}^{3+} + 2\text{H}^+ \rightarrow 2\text{H}_2\text{O} + 2\text{Ce}^{4+}$  [37, 58]. Doping of lower valence cations in nanoceria has been shown to improve  $\text{Ce}^{3+}/\text{Ce}^{4+}$  ratio, creating more oxygen vacancies and thus obtaining higher catalytic activity, decomposing  $\text{H}_2\text{O}_2$  to  $\cdot\text{OH}$ . Among doped metals including Cu, Fe ( $\text{Fe}^{2+}$  and  $\text{Fe}^{3+}$ ), Co, Zn and Mn, Cu-doped cerium oxide demonstrated the largest fraction of  $\text{Ce}^{3+}$  ( $\text{Ce}^{3+}/\text{Ce}^{4+}$  ratio Cu-doped vs naive: 0.334 vs 0.175) and highest catalytic capacity in the production of hydroxyl radicals. Advantaged from the elevated  $\text{Ce}^{3+}$  on the ceria lattice surface, near complete depletion of  $\text{H}_2\text{O}_2$  was reported. The enzyme-mimicking activity of Cu- $\text{CeO}_2$  was found to be higher than  $\text{CeO}_2$  evident by the stronger  $\cdot\text{OH}$  signals detected in the electron spin spectroscopy (ESR) spectrum [59]. Whilst many studies had showed that surface  $\text{CeO}_2$  acts as a catalytically active site and  $\text{Ce}^{3+}/\text{Ce}^{4+}$  ratio is highly correlated to the enzymatic activity of nanoceria, researchers should always experimentally verify the enzyme-mimicking activities of the engineered materials instead of making assumptions based on the measured ratio. A recent study reporting nanoceria with varying morphologies as miRNA delivery platform demonstrated that octahedral and cubic nanoceria did show a positive correlation between  $\text{Ce}^{3+}/\text{Ce}^{4+}$  with SOD and CAT activities [54]. Interestingly, the  $\text{CeO}_2$  nanorod with the highest  $\text{Ce}^{3+}$  among all formulations was found to have the lowest enzymatic activity for both SOD and CAT mimic activities [54]. The authors suspected that

the  $\text{CePO}_4$  regions from the low concentration of  $\text{Na}_3\text{PO}_4$  introduced as a mineraliser and shape control additive in the synthesis of nanorod increased the level of calculated  $\text{Ce}^{3+}$  and could diminish enzymatic activity [54].

### pH-responsive

The oxidation states of nanoceria are shown to be pH-responsive with higher efficacy of ROS production in more acidic conditions ( $\text{pH } 5.4 > \text{pH } 6.5 > \text{pH } 7.4$  [60]) and vice versa for ROS scavenging [61, 62]. Hence, the difference in acid–base status between normal and tumour tissues can be exploited and is instrumental in anticancer drug design and discovery [63]. Normal tissues interstitial pH are mostly around 7.2–7.5 under well-perfused conditions. In contrast, TME is characterised to be slightly acidic at pH 6.4–7.0 with value as low as 5.6 reported. This is due to the uncontrolled cell proliferation and high metabolic activity of tumours accompanied by insufficient blood perfusion which leads to inefficient removal of acidic metabolic waste [64–66]. Interestingly, a study demonstrated by Liu et al., whereby bare nanoenzyme cerium oxide displayed weaker catalase-like activity at pH 5.5 in comparison to a higher pH of 7.4 [67]. Nonetheless, upon encapsulation in a metal–organic framework core–shell nanohybrid system, a lower pH resulted in the conversion of  $\text{H}_2\text{O}_2$  into highly cytotoxic  $\cdot\text{OH}$  radicals that kill tumour cells with a significant increase in radicals generated when pH value decreased from 6.6 to 6.2. This study established that the encapsulation and protection of the cerium oxide core with the metal shell resulted in a ninefold

higher apoptotic efficiency in hypoxic cells than that without the shell and thus stimulating a self-feedback system through caspase-3 initiation [49, 68]. Results from a recent study demonstrated that HeLa and U87MG cancer cells exhibited > 80% cell viability after treatment at neutral pH but ~40% or less cells were viable at  $\text{pH} \leq 6.6$ , confirming enhanced toxicity in a lower pH environment [68]. The ROS scavenging/ROS generating capability under irradiation conditions of nanoceria is also pH-sensitive. Upon X-ray irradiation (total dose 5 Gy,  $1 \text{ Gy min}^{-1}$ ), a dextran-coated gadolinium-doped nanoceria  $\text{Ce}_{0.9}\text{Gd}_{0.1}\text{O}_{1.95}$  generated ROS in pH 6.0 Tris buffer but scavenged ROS, almost halving the hydrogen peroxide level in pH 8.0 Tris buffer [69].

Despite the general understanding that the oxidation states,  $\text{Ce}^{3+}/\text{Ce}^{4+}$  ratio and pH environment critically affect the redox reactions of nanoceria, very few studies provided clarification of  $\text{Ce}^{3+}/\text{Ce}^{4+}$  on the synthesised materials. The pH-responsive activities were generally assessed in cell-free assays under controlled experimental conditions, lacking the complexity and heterogeneity of physiological environments. In addition to that, there are also limited research into the oxidation states of nanoceria when the nanoparticles enter cells and reside in tissues. Szymanski first demonstrated in 2016 that a shift to a higher  $\text{Ce}^{3+}/\text{Ce}^{4+}$  was detected when nanoceria entered the cells, indicating that there was a net reduction of nanoceria in the intracellular environment [70]. A similar ratio was found in the cytoplasm and lysosomes, suggesting that the net reduction of nanoceria was an early event within the internalisation pathway [70]. Unfortunately, this was the only study that reported characterisation of nanoceria status in organelles involved in internalisation.

### Oxygen tension responsive

Hypoxia, defined as “a condition of low oxygen tension”, with  $\text{O}_2$  level typically in the range of 1–5% in comparison to normoxia sitting at 10–21% [71], is commonly found in solid tumours due to poor vascularisation in response to the unregulated proliferation and metabolism of cells starving endogenous oxygen supply [72]. Hypoxic condition is often linked to cancer progression, metastasis [73], immunosuppression [74], and limited response [75] or resistance to treatment [76], leading to poor clinical outcomes. Under the hypoxic and acidic TME, nanoceria acted as pro-oxidant to inhibit the induction of hypoxia-inducible factor 1- $\alpha$  (HIF-1 $\alpha$ ) and the subsequent oncogenic signalling pathways [77]. It was reported that HIF-1 $\alpha$  level decreased gradually over time after treatment with a 2D graphdiyne GDY– $\text{CeO}_2$  nanocomposites under both normoxic and hypoxic conditions. Nonetheless, these nanocomposites sensitized both Herceptin-sensitive and Herceptin-resistant cells whereby Herceptin treatment resulted in more potent cytotoxic

effects in cancer cells under hypoxia than under normoxia [78].  $\text{H}_2\text{O}_2$ , a relatively stable ROS, is largely produced by human tumour cells without exogenous stimulation [10]. When exposed to excess level of  $\text{H}_2\text{O}_2$ , nanoceria primarily mimicked catalase activity, increasing production of  $\text{O}_2$  over time, in contrast to no changes in  $\text{O}_2$  level detected when  $\text{H}_2\text{O}_2$  was not supplied. The generation of molecular  $\text{O}_2$  plays a key role in relieving tumour hypoxia and sensitising cancerous cells for enhanced therapeutic responses [67, 79].

Consequently, nanoceria is capable of targeting the “Triad of Death” in cancer, which consists of primary tumour growth, drug resistance and metastasis [80], through its catalytic activities that reprogram the aberrant redox environment in cancers: production of cytotoxic ROS to kill cancer cells, inhibit tumour growth and suppress the expression of pro-metastatic molecules; production of  $\text{O}_2$  to sensitise treatment-resistant cells and relieving hypoxic conditions to inhibit oncogenic signalling cascades associated with progression to metastatic disease.

### Nanoceria as potential cancer therapeutic agent

The unique properties of nanoceria that favours as an oxidising agent under acidic and hypoxic conditions, which are both key features of aggressive tumour progression, while acting as an antioxidant under physiological conditions to protect normal cells presents it as an attractive anti-cancer agent. Recent publications reporting the cancer-killing effects of nanoceria are summarised in Table 1.

### In vitro studies

Several studies have pinpointed that nanoceria exhibits anti-cancer properties through the activation of p53-dependent, mitochondrial-mediated, oxidative stress-triggered apoptosis. Nourmohammadi et al. revealed that nanoceria prepared by the co-precipitation method exerted enhanced cytotoxic effects, ROS modulation and apoptotic genes expression in fibrosarcoma cells in comparison to normal fibroblast [63, 81]. Adebayo et al. proposed that a polyacrylic acid polymer-coated nanoceria is a potential antitumorigenic agent by targeting cellular pathways linked to oxidative stress, inflammation, and apoptosis [82]. Cu-doped nanoceria with enhanced hydroxyl radicals production capability acted as pro-oxidant in cancer cells, which elevated intracellular ROS levels, resulting in a high proportion of DNA damage [59], and triggering the p53-dependent mitochondrial signalling pathway leading to cellular apoptosis. Datta reported the enhanced number of phosphorylated histone  $\gamma$ -H2AX, a marker of DNA damage, which then activated tumour suppressor

**Table 1** List of nanocerium reported to exert anti-cancer effects in 2019–2021

Nanoplatform	Size, zeta potential, morphology	Targeting moieties on NPs	Cell lines	In vitro	In vivo/ex vivo
Nanocerium [63, 81]	34.1 nm – 32.9 mV Cubic fluorite	–	Murine fibrosarcoma WEHI164 cells Normal fibroblast L929 cells	Significant cytotoxic effects on WEHI164 cells from 15.63 µg/mL ROS production in WEHI164 cells, ROS scavenging in L929 cells Number of apoptotic and necrotic WEHI164 cells increased Pro-apoptotic Bax mRNA expression upregulated in WEHI164 cells, downregulated in L929 cells	0.5 mg/kg in 100 µL PBS injected intraperitoneally twice a week for four weeks in WEHI164 tumour-bearing mice Inhibition of tumour growth Selectively accumulated in tumour No significant effects on liver and kidney functions Pro-apoptotic Bax expression upregulated, anti-apoptotic Bcl2 expression downregulated in tumours Higher number of TUNEL-positive cells per unit area in nanocerium-treated tumours indicating increased numerical density of apoptotic tumour cells
CeO <sub>2</sub> -GO <sub>x</sub> @CCM [68]	~50 nm – 20.43 mV Cubic	Coated with HeLa cancer cell membrane (CCM) for homotypic targeting	Cervical cancer HeLa cells Human umbilical vein endothelial cells HUVEC	Preferential accumulation in HeLa cells Increased ROS production in HeLa cells at slightly acidic pH ≤ 6.6 No obvious ROS production in HUVEC cells at pH 7.4	10 mg/kg in 200 µL PBS injected intravenously in HeLa tumour-bearing mice Significantly higher accumulation in tumour Complete tumour growth suppression with mice weight remained stable for 14 days High level of tumour cell apoptosis and necrosis observed in H&E stained tumour tissue No significant morphological changes observed in H&E-stained major organs

Table 1 (continued)

Nanoplatform	Size, zeta potential, morphology	Targeting moieties on NPs	Cell lines	In vitro	In vivo/ex vivo
$\text{Ce}_{0.9}\text{Gd}_{0.1}\text{O}_{1.95}$ [69]	4–6 nm Cubic	–	Breast cancer MCF-7 cells Human mesenchymal stem cells hMSC	Predominantly localised in cytoplasm and lysosomes No decrease in hMSC viability with the absence of apoptotic cells; dose-dependent decrease in viability and increase in number of apoptotic cells for MCF-7 Significantly reduced MTMP of MCF-7 cells exposed to NPs at 2.5 and 5 mg/mL Significantly increased expression levels of pro-apoptotic CD40 gene and genes related to antioxidant defence processes indicating activation of oxidative stress No significant haemolytic activity in the absence of serum proteins	

Table 1 (continued)

Nanoplatform	Size, zeta potential, morphology	Targeting moieties on NPs	Cell lines	In vitro	In vivo/ex vivo
DOX loaded HA-Cu-CeO <sub>2</sub> @CCM [59]	-Ce <sup>3+</sup> /Ce <sup>4+</sup> ratio: 0.334	Coated with MDA-MB-231 cancer cell membrane (CCM) for homotypic targeting	Breast cancer MDA-MB-231 cells Mouse myoblast C2C12 cells	Significantly higher uptake in source cancer cells Excellent hemocompatibility Near 100% killing of cancer cells resulted from the synergistic effect of DOX and Ce-CeO <sub>2</sub> Depleted DOX-induced ROS level and increased viability of C2C12 cells	5 mg/mL in 200 $\mu$ L PBS injected intravenously in MDA-MB-231 tumour-bearing mice Near complete tumour growth inhibition (98.5%) Dramatically elevated signal of superoxide indicator dihydroethidium (DHE) staining in treated tumour Down-regulated expression of proliferative marker Ki67 in the treated group H&E and TUNEL staining significantly higher proportion of DNA damage and apoptosis in tumour tissues Blood routine examination, liver and kidney function indicators and myocardium damage indicator were all in a normal range No pathological changes and significant damages in major organs observed indicating potential to relieve DOX-induced systemic toxicity
Green synthesised CeO <sub>2</sub> [105]	35–40 nm	–	HeLa cells	Dose-dependent cytotoxicity on HeLa cells when used at higher doses (50–125 $\mu$ g/mL) Cell morphology changed with more apoptotic HeLa cells observed at 100 $\mu$ g/mL	–



Table 1 (continued)

Nanoplatform	Size, zeta potential, morphology	Targeting moieties on NPs	Cell lines	In vitro	In vivo/ex vivo
CeO <sub>2</sub> [12]	1–10 nm	–	Melanoma A375 cells Normal human epidermal melanocytes NHEM	Higher basal ROS level in A375 cells that was even higher upon nanoceria treatment High level of mitochondrial O <sub>2</sub> <sup>-</sup> detected in A375 cells potentially the source for SOD-like activity of nanoceria producing H <sub>2</sub> O <sub>2</sub> Loss of MTMP induced in A375 cells Number of intermediate (0.5–5 μm) and fragmented (<0.5 μm) mitochondria increased in treated A375 cells Cell viability significantly decreased in A375 cells but preincubation with PEG-catalase fully restored the viability of treated A375 cells	–
HA-CePEI-NPs [85]	70 nm – 20 mV Spherical	Conjugated with hyaluronic acid HA to target CD44 receptor	MDA-MB-231 Human breast epithelial HBL-100 cells	Significant concentration-dependent cytotoxicity in cancer cells Loss of MTMP in cancer cells ROS levels inversely correlated with GSH levels Significantly declined Bcl-2 and elevated cytosolic Cyt c levels Dose-dependent activation of caspases-3 and -9	–

**Table 1** (continued)

Nanoplatform	Size, zeta potential, morphology	Targeting moieties on NPs	Cell lines	In vitro	In vivo/ex vivo
CeO <sub>2</sub> [83]	30–40 nm – 4.9 mV Cubic fluorite	–	Colorectal carcinoma HCT116 cells Human embryonic kidney HEK293 cells	Significantly lower IC <sub>50</sub> for HCT116 (50.48 µg/mL) than HEK293 (92.03 µg/mL) Dose-dependent increased ROS production in HCT116 Cell population in early and late apoptosis significantly increased Enhanced pro-apoptotic Bax, Bak, Cyt c, decreased anti-apoptotic Bcl2 Increased activation of caspases-3 and -9 Increased number of phosphorylated histones γ-H2AX foci Suppressed expression of Mdm2 Increased phosphorylation of p53, activation of p21 Increased DNA fragmentation	–

Table 1 (continued)

Nanoplatfrom	Size, zeta potential, morphology	Targeting moieties on NPs	Cell lines	In vitro	In vivo/ex vivo
CeO <sub>2</sub> [86]	12 nm – 14 mV Spherical Ce <sup>3+</sup> /Ce <sup>4+</sup> ratio: 0.94	–	Hepatocellular carcinoma HepG2 cells	Endocytic uptake and retention of NPs	0.1 mg/kg in 500 $\mu$ L saline solution injected intravenously in rats induced with hepatocellular carcinoma (HCC) Development of HCC nodules attenuated in the liver of treated rats Significant increase in TUNEL-positive cells in the liver of treated rats Lower macrophage infiltration measured by CD68 staining, decreased number of Ki67-positive cells in the treated group Level of phosphorylated extracellular signal-regulated kinase 1/2 (P-ERK1/2) decreased Level of linoleic acid that contributed to HCC development reversed in treated group Overall survival comparable to a group treated with tyrosine kinase inhibitor sorafenib

Table 1 (continued)

Nanopatform	Size, zeta potential, morphology	Targeting moieties on NPs	Cell lines	In vitro	In vivo/ex vivo
PN-CeO <sub>2</sub> -PSS [66]	<p>Porous nanorod: ~60.0 nm length, ~8.0 nm diameter, ~2.0–4.0 nm pore size;</p> <p>PN-CeO<sub>2</sub>-PSS—70 kDa: 306.5 nm</p>	–	<p>HepG2</p> <p>Normal human hepatic stellate LX-2 cells</p>	<p>Non-toxic to LX-2 cells at 250 µg/mL</p> <p>Dose-dependent cytotoxicity, increased caspase-3 expression in HepG2 cells under mild acidic conditions (pH 6.5)</p> <p>Apoptotic body, chromatin condensation, nucleic fragmentation and membranolysis observed in treated HepG2 cells</p> <p>Enhanced ROS and malonaldehyde (MDA) levels at pH 6.5</p>	<p>5 mg/mL in 100 µL saline solution injected intravenously in HepG2 tumour-bearing mice</p> <p>H&amp;E staining showed significant necrosis and apoptosis in treated tumour tissues</p> <p>Significant DHE staining signal observed indicating increased ROS generation in nanoceriatreated tumours</p> <p>Near complete inhibition (96.1%) of tumour growth</p> <p>Higher rate of tumour tissue apoptosis in TUNEL assay</p> <p>No significant toxicity to major organs</p> <p>No significant effects on blood biochemical indexes and liver, kidney function parameters</p> <p>No significant haemolysis</p>

p53 and disrupted ubiquitin ligase Mdm2 binding to p53 protein [83]. The increased number of phosphorylated p53 also elicited activation of its transcriptional target p21 that led to G1 or G2/M cell cycle arrest [83, 84]. Aplak et al. showed that melanoma A375 cells exhibited a significantly higher basal ROS level than their physiological counterpart NHEM cells making them more susceptible to additional oxidative provocation. The  $\text{H}_2\text{O}_2$   $\text{IC}_{50}$  value for NHEM cells (250.6  $\mu\text{M}$ ) was  $\sim 3.5$  times more than that of A375 cells (72.5  $\mu\text{M}$ ). High level of superoxide was detected in the mitochondria of A375 cells, which became the substrate for nanoceria SOD-mimetic activity producing  $\text{H}_2\text{O}_2$  [12]. The increased  $\text{H}_2\text{O}_2$  production was reported to cause the loss of mitochondrial membrane potential (MTMP) that disrupted mitochondrial structure and functions, and ultimately led to cancer cell death [12, 69]. The oxidative-stress-induced cell death was supported by the findings in which preincubation of cells with catalase that catalysed decomposition of  $\text{H}_2\text{O}_2$  into non-toxic  $\text{H}_2\text{O}$  and  $\text{O}_2$  fully rescued the cells from nanoceria-induced cytotoxicity [12]. Excess intracellular ROS depleted glutathione (GSH), depolarised mitochondrial membrane and decreased level of antiapoptotic Bcl-2 that regulates the permeability of the mitochondrial outer membrane and inhibits the release of cytochrome c (Cyt c) [83, 85]. Increased level of pro-apoptotic Bax and Bak in cytosol will be recruited to the mitochondria following stress signalling which then released Cyt c from mitochondria into cytosol [83]. Increased cytosol Cyt c level caused the activation of caspases-3 and -9 which ultimately induced programmed cell death of cancer cells [83, 85]. MDA-MB-231 cells treated with hyaluronic acid tagged nanoceria developed using oxidation method with poly(ethylenimine (PEI) showed irreversible nuclear chromatin condensation (pyknosis) and nuclear fragmentation, indicating the occurrence of nuclear apoptosis. Increase in the population of cells in the G2/M phase was also reported, revealing that nanoceria not only activated intrinsic apoptotic pathway but also reduced cell survival by preventing cells from entering mitosis and enabling the repair of DNA damage [85]. Popov et al. analysed the effects of an ultra-small dextran-coated gadolinium-doped nanoceria  $\text{Ce}_{0.9}\text{Gd}_{0.1}\text{O}_{1.95}$  on the gene expression of cancer and normal cells. Increased transcriptional activity of proapoptotic CD40 genes and a panel of antioxidant defence genes indicated activation of oxidative stress. As opposed to cancer cells, normal cells (human mesenchymal stem cells hMSCs) treated with nanoceria revealed downregulated expression of genes involved in antioxidant defence systems, antioxidant mitochondrial systems, anti-apoptotic markers, necrosis markers and proapoptotic marker BAX, indicating that cerium oxide nanozymes involved in maintaining the redox balance in hMSCs [69].

## In vivo studies

Several studies have reported investigating the biosafety and therapeutic efficacies of nanoceria in tumour models. Fernández-Varo et al. demonstrated that the antioxidative and anti-inflammatory properties of a 4–5 nm nanoceria synthesised by the co-precipitation method can partially revert cell mechanisms involved in tumour progression and significantly improved survival in Wistar rats bearing hepatocellular carcinoma (HCC). Decreased macrophage infiltration, and decreased levels of phosphorylated extracellular signal-regulated kinase 1/2 (P-ERK1/2) related to stress-responsive Ras/MAPK signalling pathway were reported. Nanoceria also restored fatty acids metabolism that was found to be dysregulated in HCC animals as highly proliferative cancer cells demonstrate strong lipid and cholesterol activity to support proliferation [86]. Levels of malondialdehyde MDA (end-product of lipid peroxidation), myeloperoxidase MPO activity (lysosomal oxidising agent) and nitric oxide (inflammatory marker), that were significantly increased in Wistar rats bearing breast tumours, were ameliorated in rats treated with nanoceria [82]. The exact mechanisms in which nanoceria is affecting lipid and cholesterol metabolisms require further study and could provide insights into potential applications of nanoceria in other diseases that arise from dysregulated lipid and cholesterol activities.

The cancer therapeutic potential of nanoceria was investigated in preclinical disease models. Tian et al. reported 51.1% shrinking of tumour weight with intravenously administered porous cerium oxide nanorod prepared via the hydrothermal method and the anti-cancer effect of nanoceria was enhanced to 96.1% with sodium polystyrene sulfonate coating [66]. Intraperitoneally administration of 0.5 mg/kg of a  $\sim 32$  nm nanoceria with negative surface charge ( $-26.3$  mV) suppressed the growth of WEHI164 tumour [81]. A copper-doped nanoceria showed near complete inhibition of tumour growth (98.5% inhibition) [59]. Tumour growth was inhibited as indicated by the significant down regulation of proliferation marker Ki67 of MDA-MB-231 tumour in mice [59] and HCC in rats [86]. Hematoxylin and eosin (H&E) staining revealed a larger density of necrotic and apoptotic cells in treated tumour tissue sections in contrast to the control group [59, 66, 68]. Terminal deoxynucleotidyl transferase dUTP nick end-labeling (TUNEL) staining of tumour tissue sections showed a higher proportion of DNA damage in nanoceria-treated tumours, suggesting enhanced tumour cell apoptosis [59, 81]. Apoptotic marker genes pro-apoptotic Bax and caspase-3 that are involved in the apoptotic pathway were significantly increased in nanoceria-treated tumours whilst expression of anti-apoptotic Bcl2 was downregulated [66, 81]. Elevated signal from superoxide marker dihydroethidium (DHE) staining

of tumour tissues [59, 66, 81] also demonstrated increased ROS production *in vivo* upon nanoceria treatment to trigger oxidative stress-induced cell apoptosis.

In summary, a considerable amount of research outputs from *in vitro* and *in vivo* studies had inferred that nanoceria of various surface characteristics and functionalisation is capable of attenuating tumour growth through inducing programmed cell death in preclinical models and the efficacy is significantly enhanced with surface modifications of nanoceria. With the large variety of methodologies for surface coatings and functionalisation available in the preparation of nanomaterials [52, 53, 87], there is an urgent need in developing a clinically relevant pipeline in the rational design of surface modifications on nanoceria to accelerate the development of potent nanoceria formulations, ensure that the nanoparticles prepared are fit for need and to identify biomolecules as robust, specific biomarkers for monitoring responses to nanoceria administration.

## Nanoceria in metastatic diseases

Activating invasion and metastasis being the hallmark of cancer have been responsible for the majority of cancer-related deaths as the complexity of metastatic progression poses hurdles in the development of efficacious therapeutic approaches, resulting in poor prognosis in advanced cancers [88–90]. Whilst still in the nascent stage of studies, the anti-angiogenic effect of nanoceria could potentially play a role in tumour growth suppression as angiogenesis, another cancer hallmark, is known to be involved in promoting tumour vascularisation and metastasis [91]. Giri et al. first reported in 2013 that treatment with  $\text{Ce}^{3+}$  dominating nanoceria of ~38 nm hydrodynamic radius inhibited migration and invasion of ovarian cancer SKOV3 cells through inhibition of growth factors including stromal cell-derived factor 1 SDF1, heparin-binding EGF-like growth factor HB-EGF and vascular endothelial growth factor VEGF [92]. Metastatic nodules were significantly reduced in size and decreased in numbers in the lungs of nanoceria-treated mice. Tumour xenograft slides were stained with TUNEL to detect cells undergoing apoptosis and CD31 to identify endothelial cells in microvessels. Co-localisation of stains was observed suggesting that nanoceria could contribute to anti-angiogenic effects by inducing apoptosis of endothelial cells in microvessels. Xiao et al. then demonstrated that nanoceria prepared by the thermal decomposition method with 3 nm core size and -18 mV surface charge could suppress the metastatic potential of gastric cancer cells BGC823 and MKN28 [93]. Cancer cells were pre-treated with or without nanoceria before being injected intraperitoneally into nude mice every 3 days. Less metastatic tumours were observed in nanoceria-treated group than there were in the

control mice injected with cancer cells that were not co-cultured with nanoceria [93]. Hao et al. treated Herceptin-resistant Pool2-nGL tumours implanted into the mammary fat pads of the mice with nanoceria plus Herceptin. The researchers observed significantly decreased expression of Ki67, VEGF and CD31, suggesting that the combination treatment could suppress tumour growth and metastasis [77]. Recently, Yong et al. reported that nanoceria with a particle diameter of 5–6 nm decreased the expression of hypoxic angiogenic genes HIF-1 $\alpha$  and VEGF-A in human melanoma Me1007 cells [40]. VEGF is upregulated by HIF-1 $\alpha$  during hypoxia that induces the development of blood vessels in solid tumours and promotes intravasation of cancer cells from primary tumour sites [94].

Zuo et al. established an experimental metastasis model by intravenous injection of melanoma B16F10 cells into tail vein of C57BL/6 mice at day 5 after subcutaneous injection of the melanoma cells [32]. Treatment with a nanoceria-based nanoplatform (IR-780 and metformin-loaded mesoporous silica nanoparticles with nanoceria as gatekeepers) reduced the number of metastatic nodules on the lung surface in comparison to the control group. Expression of N-cadherin was decreased whereas E-cadherin was increased in the tumour tissues exposed to nanoparticles indicating anti-metastatic potential of the nanoplatform [32]. Cadherins are involved in the epithelial-to-mesenchymal transition (EMT) which enhanced the mobility and invasion capabilities of cancer cells that elevated N-cadherin level is reported to promote metastatic behaviour of tumour cells [95] whilst expression of E-cadherin is believed to suppress tumour growth and metastasis [96]. Infiltration of myeloid-derived suppressor cells (MDSCs) in tumour sites under hypoxia via the HIF-1 $\alpha$  pathway [97] was significantly reduced in treated tumours [32]. The reduction in MDSC recruitment resulted in a decreased inhibitory effect on T cells and down-regulated immune checkpoint programmed death ligand 1 PD-L1 expression [32] which could reverse MDSC-mediated immunosuppression to enhance therapeutic outcomes of immunotherapy treatment and inhibit MDSC involvement in the formation of premetastatic niches, tumour angiogenesis and tumour cell invasion [98]. Zhu et al. investigated a ruthenium-loaded cerium oxide yolk shell nanozymes Ru@CeO<sub>2</sub>-RBT/Res-DPEG for dual chemotherapy/photothermal therapy in orthotopic CT26 colorectal cancer model [99]. The combined treatment resulted in significantly reduced metastasis in intestine with no detectable metastases in liver, spleen, and lung when all mice in the control group has extensive metastases observed.

Liu et al. proposed the use of a homologous targeted nanoceria integrated with dendritic mesoporous silica nanoparticles as neoadjuvant chemotherapy to inhibit metastases of breast cancer without significant systemic toxicity [100]. *In vitro* wound-healing assay, Transwell invasion assay and

increased expression of DHX15 that inhibit the intrinsic invasive and metastatic ability of cancer cells [101] revealed the metastatic inhibitory effect of engineered nanoceria in 4T1 cells [100]. Liu also demonstrated the nanoceria prepared effectively hindered the transdifferentiation of fibroblast to cancer-associated fibroblast (CAF) and reprogrammed CAF back to a normal fibroblast both in vitro and in vivo [100]. CAF is shown to modulate cancer metastasis and has thus attracted great interests as a therapeutic target [102, 103]. Whilst the nanoparticles alone did not exert anti-cancer effects on the primary tumour, pre-treatment with intravenous injection of 1 mg/kg nanoceria coupled with 3 mg/kg doxorubicin (DOX) every 3 days for 4 times resulted in effective tumour growth control. Primary tumours were removed 25 days post inoculation and another 3 times of treatment were administrated as post-surgical management. The number of lung metastasis and liver metastasis modules observed were significantly reduced in nanoceria treated orthotopic 4T1 breast cancer model [100].

In contrast to reported metastatic suppressive effects, naïve nanoceria has also been shown to not exert effective anti-metastatic activity but instead work synergistically with other bioactive drugs. Naz revealed that metastatic lung cancer A549 cells migrated from the invasion chamber to the lower feeder upon treatment with nanoceria in comparison to nanoceria incorporated with lactonic sophorolipids and ganetespib that dramatically decreased the migratory ability of the cells [104].

In summary, nanoceria potentially inhibits metastatic progression in different stages through decreasing cell survival and proliferation, attenuating expression of molecules that are associated with epithelial-to-mesenchymal transition, angiogenesis and vascularisation, or alternatively as neo-adjuvant or adjuvant treatment to sensitise the tumour cells for enhanced therapeutic efficacies of conventional systemic therapies. Further studies could consider the potential of nanoceria as maintenance therapy upon primary treatment to manage the risk of developing metastatic disease.

## Sensitisation of cancer cells for therapies

Apart of direct inhibition of primary tumour growth, nanoceria also assists in combatting drug/treatment resistance through sensitisation of cancer cells to enhance treatment responses. Nanoceria with the ability to generate molecular oxygen in TME is widely exploited as sensitising agents in photodynamic, photothermal and radiation therapies (Table 2). The incorporation of nanoceria with conventional drugs also demonstrated the potential to rectify resistance in targeted and chemo-therapies.

## Photodynamic therapy

Photodynamic therapy (PDT) being a promising non-invasive adjuvant anti-cancer treatment requires photosensitisers that transform light energy from an irradiation source into other forms that kill cancer cells. PDT effectively destroys tumours by energising photosensitisers at a specific wavelength, which triggers photochemical reaction utilising endogenous molecular oxygen ( $O_2$ ) as substrate in the production of cytotoxic ROS molecules [75, 106]. However, the limited photodynamic reaction of photosensitisers have been reported due to the  $O_2$  deprivation at tumour sites [67, 79]. Thus, nanoceria-based therapeutics with the capability to catalyse  $O_2$  accumulation within cancerous tissues are developed as effective photosensitising agents.

Liu's group reported a functionalised nanoceria in a metal-organic framework acting as PDT sensitiser, inducing apoptosis in hypoxic tumour cells upon laser irradiation through a tandem homogenous catalysis process: decomposition of  $H_2O_2$  to  $O_2$  relieving hypoxia followed by conversion of  $O_2$  to cytotoxic ROS. Additionally, the nanosystem was engineered with Cy3-labelled peptide which was cleaved by caspase-3 activated in apoptotic events, achieving in situ monitoring of therapeutic response [67]. A  $CeO_2$  nanozyme system loaded with photosensitiser indocyanine green (ICG) improved the killing of MCF-7 cells in comparison to free ICG as  $CeO_2$  increased intracellular ROS that induced cell death, in addition to the thermal effects of ICG upon laser irradiation. Blood oxygen saturation level was significantly improved, and hypoxia signal was substantially reduced in tumours, suggesting that the  $CeO_2$  NPs acted as artificial enzymes catalysing the production of  $O_2$  from  $H_2O_2$ . Ex vivo analyses revealed severe tissue apoptosis and complete disappearance of tumours without recurrence in any location (Fig. 3) [79]. Zhang et al. reported a  $CeO_2$  nanoclusters loaded with weak PDT photosensitiser Cy5 that with near-infrared (NIR) illumination,  $Cy5 + CeO_2$  demonstrated higher cytotoxicity in hepatic carcinoma cells than Cy5 alone [107]. This indicated that the decomposition of  $H_2O_2$  to  $O_2$  by  $CeO_2$  became the raw material and photochemical reaction driving force for Cy5 to convert  $O_2$  to  $\cdot OH$  radicals.

Zuo et al. successfully synthesised a mesoporous silica nanoparticles (MSNs) loaded with photosensitiser IR780, mitochondrial respiration inhibitor Metformin (Met) and  $CeO_2$  NPs ( $CeO_2@MSNs@IR780/Met$ ) [32]. The nano-platform promoted tumour oxygenation through  $CeO_2$ 's  $O_2$  generation and Met's  $O_2$  economisation, enhanced IR780's capability of generating toxic singlet oxygen from molecular oxygen. It is worthy to note that alleviating tumour hypoxia also attenuated the recruitment of myeloid-derived

**Table 2** Summary of nanoceria-based nanoplatform engineered to sensitise tumour cells for enhanced photodynamic PDT, photothermal PTT and radiation therapeutic effects

Nanoplatform	Sensitiser	Targeting moieties on NPs	Cancer cell line	In vitro	In vivo and ex vivo	Treatment protocol
CeO <sub>x</sub> @FMIL [67]	CeO <sub>x</sub>	Labelled with folic acid FA to target folate receptors	HeLa	Signal of cell-permeable hypoxia indicator significantly reduced Strong singlet oxygen sensor green signal generated upon laser irradiation	–	Irradiation with 660 nm laser (200 mW/cm <sup>2</sup> ) for 5 min, 6 h post treatment (in vitro)
ICG@PEI-PBA-HA/CeO <sub>2</sub> [79]	Indocyanine Green ICG Ce <sup>3+</sup> /Ce <sup>4+</sup> ratio: 0.85	Hyaluronic Acid HA conjugation to target CD44 receptor	MCF-7	Intracellular ROS increased Cancer cell killing enhanced with ICG-CeO <sub>2</sub> + laser compared to ICG + laser	Blood oxygen saturation increased from ~30% basal level to ~80% 24 h after IV injection Tumour hypoxia signals significantly reduced Tumours completely destroyed after treatment with nanomaterials and PTT, no sign of recurrence Severe tumour tissue apoptosis observed with TUNEL staining	100 µg/mL ICG in 100 µL injected intravenously into MCF-7 tumour-bearing mice Irradiation with 808 nm laser (1 W/cm <sup>2</sup> ) for 4 min, 24 h post-injection (in vivo)
CeO <sub>2</sub> @DNA-DOX [107]	Cy5	DNA sequence complementary to target miRNA-21	HePG2	In absence of laser, intracellular H <sub>2</sub> O <sub>2</sub> cleared by CeO <sub>2</sub> to produce O <sub>2</sub> After NIR illumination, weak endogenous PDT ability of Cy5 enhanced with increasing production of highly toxic ·OH from accumulated O <sub>2</sub>	–	Irradiation with 625 nm laser for 30 min-1 h (in vitro)



Table 2 (continued)

Nanoplatform	Sensitiser	Targeting moieties on NPs	Cancer cell line	In vitro	In vivo and ex vivo	Treatment protocol
CeO <sub>2</sub> @MSNs@IR780/ Met [32]	IR780	No targeting ligand, redox responsive CeO <sub>2</sub> as gatekeepers for release of drugs at H <sub>2</sub> O <sub>2</sub> rich tumour site	Murine melanoma B16F10 cells	Significant toxic singlet oxygen generated by IR780 from simultaneous generation and economisation of O <sub>2</sub>	H&E staining of treated tumours demonstrated cell integrity destroyed with massive apoptotic bodies Decreased number of Ki67-positive cells indicating tumour cell proliferation inhibited TUNEL staining revealed distinct apoptosis in treated tumour tissues Survival rate of mice extended from 0% in control group to 75% in treated group Metastatic mouse model demonstrated reduced numbers of metastatic nodules on lung surface in treated mice Decreased expression of N-cadherin that promotes tumour metastasis and increased expression of E-cadherin that is anti-metastatic Tumour oxygenated (strong oxygenated haemoglobin signal) Ex vivo HIF-1 $\alpha$ staining, protein and mRNA levels of HIF-1 $\alpha$ in tumour tissues were all decreased in the treated group	16 mg/kg Met, 20 mg/kg IR780 injected into B16F10 tumour-bearing mice Irradiation with 808 nm laser (1 W/cm <sup>2</sup> ) for 5 min (in vitro); 10 min, 8 h post-injection (in vivo)

Table 2 (continued)

Nanoplatform	Sensitiser	Targeting moieties on NPs	Cancer cell line	In vitro	In vivo and ex vivo	Treatment protocol
CeO <sub>2</sub> -PEG-Ce6-GOx (CPCG) [108]	Chlorin e6 Ce6	-	HeLa	Laser-induced cytotoxicity greater than free Ce6 and CFC (NP without glucose oxidase GOx) Large amount of ROS produced Significant cytotoxicity upon laser irradiation	Negligible systemic toxicity PDT/starvation treatment group demonstrated the most significant tumour growth inhibition	1.5 mg/mL CPCG in 100 $\mu$ L injected intratumourally into HeLa tumour-bearing mice Irradiation with 660 nm laser (0.2 W/cm <sup>2</sup> ) for 6 min (in vivo)
CeO <sub>x</sub> -EGPLVGRGK-PPa [58]	Pyropheophorbide-a PPa Ce <sup>3+</sup> /Ce <sup>4+</sup> ratio: 0.25	EGPLVGRGK substrate peptide of matrix metalloproteinase-2 (MMP-2)	HePG2	Nanoprobe endocytosed, peptide cleaved by endogenous MMP-2 to release PPa Large amount of ROS produced upon laser irradiation Dose-dependent cytotoxicity under irradiation indicating excellent PDT efficacy	-	Irradiation with 660 nm laser for 5 min (in vitro)
ATP-HCNPs@Ce6 [117]	Ce6 Ce <sup>3+</sup> /Ce <sup>4+</sup> ratio: 1.7:1	-	Murine mammary carcinoma cells 4T1	ATP improved stability and biocompatibility of NPs Co-localisation of NPs and lysosomes Enhanced PDT phototoxicity Higher intracellular oxygen generated in presence of H <sub>2</sub> O <sub>2</sub>	80% tumour volume reduction in ATP-HCNPs@Ce6 + PDT H&E staining revealed larger areas of cell death and inflammatory infiltration in treated tumour tissues H&E staining showed no significant damage to vital organs	50 $\mu$ M Ce6 in 20 $\mu$ L injected intratumourally into 4T1 tumour-bearing mice Irradiation with 660 nm laser (0.05 or 0.2 W/cm <sup>2</sup> ) for 5 min, 2 h post-injection (in vivo)

Table 2 (continued)

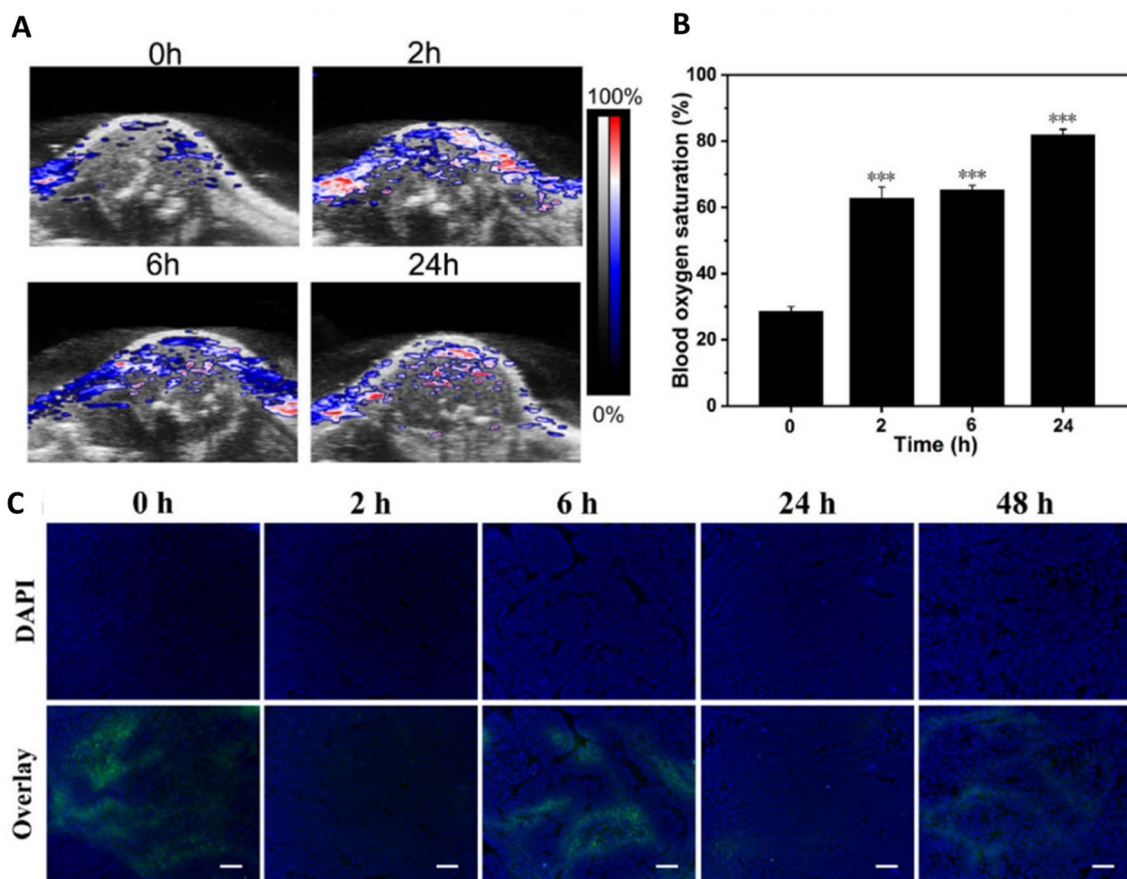
Nanoplatform	Sensitiser	Targeting moieties on NPs	Cancer cell line	In vitro	In vivo and ex vivo	Treatment protocol
MCSCe [110]	Carbon nanosphere (CS) Ce <sup>3+</sup> /Ce <sup>4+</sup> ratio: 0.96	4T1 cancer cell membrane coating for homotypic targeting	4T1	SOD-like activity catalysed transformation of intracellular superoxide into H <sub>2</sub> O <sub>2</sub> Accumulated intracellular H <sub>2</sub> O <sub>2</sub> decomposed to ·OH through NIR-activated thermal catalysis Homologous targeting, higher uptake and enhanced NIR irradiation-induced cytotoxicity in cancer cells MTMP declined and mitochondrial dysfunction indicative of cell apoptosis	Preferential accumulation of nanomaterials at tumour sites Local hyperthermia with temperature increased to ca. 55 °C upon irradiation Improved therapeutic effect with nanoceria formulated treatment (MCSCe + laser) compared to carbon nanosphere (MCS + laser) Significant apoptosis/necrosis observed in H&E and TUNEL stained tumour tissues from treated group ~90% injection dose cleared in 1 week H&E staining, liver and kidney function markers, serum biochemical and haematological parameters of treated groups all were similar to the control group and fell within normal ranges	20 mg/kg MCSCe in 100 µL PBS injected intravenously into 4T1 tumour-bearing mice Irradiation with 808 nm laser (1.5 W/cm <sup>2</sup> ) for 8 min, 24 h post-injection (in vivo)
NCeO <sub>2</sub> -PEI-MoS <sub>2</sub> [111]	Molybdenum sulphide MoS <sub>2</sub>	-	MDA-MB-231	Intracellular ROS generation upon laser treatment increased as a function of nanoceria concentration up to 0.5 mg/mL >90% cytotoxicity under laser light irradiation at 0.25 and 0.5 mg/mL nanoceria	-	Irradiation with 808 nm laser (0.5 W/cm <sup>2</sup> ) for 5 min (in vitro)

Table 2 (continued)

Nanoplatform	Sensitiser	Targeting moieties on NPs	Cancer cell line	In vitro	In vivo and ex vivo	Treatment protocol
CNPs@( $g-C_3N_4/CeO_x$ )-Met [112]	$g-C_3N_4$	-	HepG2	<p>NPs slowly penetrated into the center of 3D spheroid tumour cell model and released <math>g-C_3N_4</math> after 4 h</p> <p>Temperature rose and remained above 42 °C for PTT</p> <p>Complete killing of cells with synergistic PTT/PDT</p> <p>Enhanced ROS production that depleted GSH to reduce oxidation resistance against PDT procedure</p>	<p>Temperature rose to 42.1 °C and photothermal conversion ability remained stable after 5 cycles of laser irradiation</p> <p>PET imaging revealed alleviation of tumour hypoxia by NPs, not by oxygen supply from blood vessels</p> <p>Significant inhibition of tumour growth and longer survival period with combined PTT/PDT</p> <p>Higher degree of necrosis and apoptosis observed from H&amp;E staining of treated tumour tissues</p> <p>Intensity of cell proliferative marker Ki67 and hypoxia marker HIF-1<math>\alpha</math> signals declined</p> <p>No significant H&amp;E pathological variations observed in vital organs of treated mice in comparison to the control group</p> <p>Haematology assays indicated no acute toxicity to mice</p>	<p>5 mg/mL nanomaterials in 100 <math>\mu</math>L injected intravenously into HepG2 tumour-bearing mice</p> <p>Irradiation with 808 nm laser (0.5 W/cm<sup>2</sup>) for 10 min (in vitro); 8 min for PTT, 15 min for PTT/PDT, 12 h post-injection (in vivo)</p>

Table 2 (continued)

Nanoplatfrom	Sensitiser	Targeting moieties on NPs	Cancer cell line	In vitro	In vivo and ex vivo	Treatment protocol
$\text{Bi}_2\text{S}_3@ \text{Ce6}-\text{CeO}_2$ [113]	$\text{Bi}_2\text{S}_3$ (PTT) Ce6 (PDT)	-	4T1	Enhanced ROS production with $\text{CeO}_2$ formulated NPs Intracellular $\text{H}_2\text{O}_2$ consumed by $\text{CeO}_2$ to produce cytotoxic $^1\text{O}_2$ PDT/PTT combination treatment nearly ablated all cancer cells Real-time cellular analysis revealed effective PDT/PTT effects in inhibiting cancer cell growth	Tumour temperature rose to $60.6^\circ\text{C}$ upon injection and irradiation, but no significant temperature change in other tissues PDT or PTT alone inhibited tumour growth to some extent Near complete tumour eradication with PDT/PTT combination treatment TUNEL staining revealed most extensive necrosis in the NPs+PDT/PTT treatment group Immunohistochemistry staining showed NPs+PDT/PTT treatment damaged CD31-positive tumour microvessels and inhibited number of Ki67-positive proliferating cells	2 mg/mL NPs in 50 $\mu\text{L}$ injected intratumourally into 4T1 tumour-bearing mice Irradiation with 660 nm laser ( $0.2 \text{ W/cm}^2$ ) for 2 min or 808 nm laser ( $1.5 \text{ W/cm}^2$ ) for 3 min
GDY- $\text{CeO}_2$ -miR181a-PEG-iRGD [78]	$\text{CeO}_2$ and miR181a	iRGD peptide that mediates binding to neuropilin-1 receptor upon proteolytic activation	Human esophageal cancer cells ESCC (KYSE30 and KYSE180)	HIF-1 $\alpha$ protein level in KYSE30 cells decreased gradually under normoxia and hypoxia Radiation-induced DNA damage and apoptosis enhanced in KYSE30 and KYSE180 cells	Radiosensitivity enhanced in KYSE30 tumour-bearing models and patient-derived xenograft models evident by the significant inhibition in tumour growth	Intravenous injection of nanocomposites to ESCC patient-derived xenograft model 6 or 12 Gy X-ray radiation (repeat injection + irradiation) after injection



**Fig. 3** MCF-7 tumour-bearing BALB/c-nude mice injected with 100  $\mu\text{L}$  of ICG@PEI-PBA-HA/CeO<sub>2</sub> (including 1 mg/mL HA/CeO<sub>2</sub>) through the tail vein. **a** Photoacoustic images of tumour blood oxygen saturation levels and **b** average saturation levels shown by photoacoustic images at different times after intravenous injections demonstrated significant improvement in blood oxygen saturation level in

hypoxic tumours. **c** Representative tumour hypoxia immunofluorescence images revealed substantially reduced tumour hypoxia signals after administration of ICG@PEI-PBA-HA/CeO<sub>2</sub> (the scale bar is 50  $\mu\text{m}$ ). Reprinted with permission from [79]. Copyright 2020 American Chemical Society

suppressor cells which mediated immunosuppression and contributed to low response to antitumour immunotherapy [32, 74]. A nanocomposite consisted of PEG-functionalised CeO<sub>2</sub>, photosensitiser chlorin e6 (Ce6) and glucose oxidase (GOx) was synthesised for enhanced PDT through sequential catalytic reactions involving dual-path modulation of H<sub>2</sub>O<sub>2</sub>. CeO<sub>2</sub> transformed superoxide anion into H<sub>2</sub>O<sub>2</sub> and GOx decomposed glucose into H<sub>2</sub>O<sub>2</sub>. CeO<sub>2</sub> then catalysed the generation of O<sub>2</sub> from the accumulated H<sub>2</sub>O<sub>2</sub>. As glucose consumption by GOx requires O<sub>2</sub>, the O<sub>2</sub> supplied by CeO<sub>2</sub> enhanced the glucose depletion that impeded nutrient supply and starved the tumour cells for a synergistic photodynamic/starvation treatment [108]. Whilst authors claimed that NPs resulted in significant tumour inhibition, this study did not perform any histological examination of extracted tumours nor further analysis of biomarkers. This study only looked at the relative tumour volume to assess therapy efficacy and did not include vital information such as the frequency of NP administration.

Fan et al. successfully engineered a stimulus-responsive cerium oxide-based nanoprobe (CeO<sub>x</sub>-EGPLGVRGK-PPa) that is selectively activated in cancer cells for efficient PDT. The octahedral nanoceria with Ce<sup>3+</sup>/Ce<sup>4+</sup> of 0.1/0.9 demonstrated a more effective catalase-mimicking activity relieving tumour hypoxia. Nanoceria with a wide absorption spectrum from 300 to 1200 nm was utilised as the acceptor of the Förster resonance energy transfer (FRET) effect that quenched the PPa's fluorescence during the "silent state". Matrix metalloproteinase-2 (MMP-2) overexpressed in cancer cells will cleave the peptide EGPLGVRGK off to activate the nanoprobe at the tumour site, resulting in PPa restoring its fluorescence and producing toxic singlet oxygen <sup>1</sup>O<sub>2</sub> upon 660 nm light irradiation [58].

### Photothermal therapy

Photothermal therapy (PTT) is another promising phototherapy that utilises photosensitisers to convert NIR light

into heat energy, creating localised elevated temperature that kill tumour cells through cancer cell membrane destruction, tumoral DNA denaturation and blocking of angiogenesis. However, PTT faces drawbacks with insufficient heat generation at disease sites and thermal damage to surrounding tissues [75, 109]. Thus, nanozymes like nanoceria are incorporated into the design of PTT nanomaterials for targeted local hyperthermia and to protect normal tissues from collateral damage.

Zhang synthesised a cerium-dotted carbon nanosphere (MCSCe) that utilised nanoceria with  $\text{Ce}^{3+}/\text{Ce}^{4+}$  ratio of 0.49/0.51 for its SOD-like activity to decompose superoxide to  $\text{H}_2\text{O}_2$ . The carbon nanosphere formed hyperthermia upon NIR irradiation, which then catalysed the production of  $\cdot\text{OH}$  radicals from  $\text{H}_2\text{O}_2$  under heat stress [110]. Murugan reported a molybdenum sulphide nanoflakes ( $\text{MoS}_2$ ) decorated with nanoceria that improved the photoconversion efficiencies of the photothermal agent  $\text{MoS}_2$ . When irradiated with laser light, bare  $\text{MoS}_2$  flakes showed a temperature increase of up to 41.8 °C, whilst  $\text{MoS}_2$  flakes decorated with 0.25 and 0.5 mg/mL nanoceria enhanced the heat generation ability, with temperature increase up to 53.7 and 47.6 °C, respectively. These nanoceria- $\text{MoS}_2$  formulations also showed enhanced photostability with consistent heating-cooling profiles of the nanoflakes when irradiated repeatedly for five laser on/off cycles [111].

### Photodynamic/photothermal therapy

Jiang et al. reported multifunctional,  $\text{H}_2\text{O}_2$ -sensitive and  $\text{O}_2$  self-regenerative UCGM NPs ( $\text{CNPs}@(\text{g}-\text{C}_3\text{N}_4/\text{CeO}_x)\text{-Met}$ ) as a potential PDT/PTT agent. Catalase-mimicking nanoceria oxidised  $\text{H}_2\text{O}_2$  into  $\text{O}_2$  and Met inhibiting cellular respiration alleviated the hypoxic condition in deep tumour tissues. Results attained demonstrated no significant changes in the blood vessels of tumour-bearing mice thus indicating that the tumour hypoxia was relieved by the administration of NP. Accumulated  $\text{O}_2$  then detached photosensitiser  $\text{g}-\text{C}_3\text{N}_4$  that penetrates to the core of the tumour tissue. Upon exposure of 808 m laser, the NPs with upconversion ability will emit short wavelength laser, exciting  $\text{g}-\text{C}_3\text{N}_4$  to generate toxic ROS. Additionally, UCGM NPs displayed excellent performances in upconversion luminescence (UCL), MR and CT imaging that can be exploited for imaging-guided drug delivery system [112]. Zeng et al. synthesised  $\text{Bi}_2\text{S}_3@\text{Ce6}-\text{CeO}_2$  with  $\text{Bi}_2\text{S}_3$  as PTT agent and as photoacoustic (PA) and computed tomography (CT) contrast agent, Ce6 as a photosensitiser for PDT and  $\text{CeO}_2$  as  $\text{O}_2$  evolving-agent.  $\text{CeO}_2$  converted  $\text{H}_2\text{O}_2$  into  $\text{O}_2$  which then was converted to toxic singlet oxygen through Ce6-mediated photodynamic reaction. The NPs itself

did not exert any toxic effects both in vitro and in vivo, indicating excellent biocompatibility and biosafety. However, upon irradiation with 660 nm (PDT) or 808 nm (PTT) laser alone, significant anti-cancer effects were observed. The synergistic combination of PDT followed by PTT demonstrated near complete eradication of tumour [113].

### Radiation therapy

Zhou et al. designed a 2D graphdiyne (GDY) immobilised ultrasmall  $\text{CeO}_2$  nanozymes, loaded with microRNAs ( $\text{GDY}-\text{CeO}_2\text{-miR181a-PEG-iRGD}$ ) to overcome tumour radioresistance and enhance radiotherapy efficacy in oesophageal squamous cell carcinoma. Nanoceria relieving tumour hypoxia and miR181a directly targeting RAD17 (checkpoint protein for DNA repair, upregulated in radioresistant cells) acted as radiosensitisers, enhanced the intracellular radiation energy deposition which resulted in DNA damage of cancer cells [78].

### Targeted therapy

Hao et al. proposed the use of nanoceria to sensitise Herceptin-resistant HER2+ breast cancer cells to Herceptin therapy, which is a monoclonal antibody targeting epidermal growth factor receptor 2 (HER2) proto-oncogene found overexpressed in 20–25% of breast tumours [77, 114]. While the employment of nanoceria alone did not demonstrate significant killing of cancer cells in vitro, Herceptin and nanoceria together exhibited an enhanced inhibition on survival and proliferation of Herceptin-resistant cells under hypoxia than under normoxia. Hence, nanoceria potently blocked the induction of HIF-1 $\alpha$  to VEGF signalling pathway under hypoxia which is associated with aggressive tumour progression and metastasis [77, 115].

### Chemotherapy

Wu et al. discovered that pre-treating lung cancer A549 cells with low dose (10  $\mu\text{g}/\text{mL}$ ) hydrothermally prepared nanoceria exhibiting uniform sheet-like shapes (50 nm thickness) enhanced the anti-cancer efficacy of chemotherapeutic agent DOX through the disruption of mitochondrial function and impairment of DOX detoxification. Nanoceria triggered ROS production which severely depolarised mitochondrial membrane and consumed intracellular GSH that typically initiated drug detoxification. Nanoceria pre-treated cells demonstrated depletion of ATP required to support drug pump activity, resulting in the restricted efflux of DOX (31.3% vs 59.3% drug loss in pre-treated vs non-treated cells) [116].

## Synergistic anticancer effects

Nanoceria in combination with other anti-cancer agents, have shown to demonstrate synergistic cancer-killing activities. Wang et al. reported a Ce doped Cu–Al layered double hydroxide ultrathin nanosheets loaded with photothermal agent ICG as an integrated synergistic chemodynamic (CDT) and photothermal (PTT) therapeutic agent. The nanocomposite first catalysed  $\text{H}_2\text{O}_2$  decomposition to  $\cdot\text{OH}$  radicals, and in the presence of oxidised cerium and copper ions, depleted intracellular reducing agent GSH which is a potent  $\cdot\text{OH}$  scavenging agent. The GSH-reduced metal ions catalysed further Fenton reaction generating toxic radicals, enhancing CDT efficacy. The production of cytotoxic ROS was boosted by hyperthermia from laser irradiation of ICG-loaded nanocomposite that the combination index (CI) was determined to be less than 0.8 (Synergism:  $\text{CI} < 1$  [118]). Advantaging from its strong NIR absorption and paramagnetic Cu(II), the nanocomposite showed excellent dose-dependent photoacoustic (PA) and magnetic resonance (MR) imaging performance [60]. Dong and group synthesised a cerium-based nanozyme (PEG/Ce-Bi@DMSN) with PTT capability. Near-infrared illumination resulting in local hyperthermia enhanced the POD- and CAT-mimicking catalytic activities, and GSH consumption of nanoceria. Significantly stronger anti-cancer effects and higher survival rate were achieved with PEG/Ce-Bi@DMSN + laser in U14 tumour-bearing mice. The presence of element Bi in the nanocomposite also allowed in vivo high-contrast computed tomography (CT) imaging [119].

## Nanocarrier to improve drug delivery

Advantaging of the nanoscale size, nanoceria has been used in cancer treatment as a nanocarrier to enhance the bioavailability of anticancer agents by improving their solubility, stability and circulating half-life. Chen et al. fabricated a  $\text{CeO}_2$ @ $\text{SiO}_2$ -PEG nanoplatform as a potential drug delivery carrier for both hydrophilic and hydrophobic drugs [120]. Naturally derived bioactive polyphenols curcumin and quercetin complexed with cerium significantly decreased the viability of MDA-MB-231 and A375 cells upon blue light irradiation in comparison to free compounds. Significant changes in cell morphology with increased programmed cell death indicated that cerium complexation could overcome the low solubility of curcumin and rapid elimination of quercetin which then enhances their PDT capability [121]. Zhlobak synthesised a nanoceria-curcumin composite that significantly reduced the autoxidative degradation rate and inhibited UV-induced photodegradation of curcumin through the inactivation of ROS. When treated with nanoceria-curcumin and UVC (253.7 nm) irradiation,

enhanced cytotoxic effects were observed in tumour cells whilst normal cells were protected against the short-wave UV irradiation [122]. Nanoceria functionalised with targeting ligand also allows targeted delivery of two or more drugs for enhanced therapeutic effects. Naz et al. reported a folate-conjugated nanoceria coloaded with potential anticancer drug lactonic sophorolipid (LSL) and Hsp90 inhibitor ganetespib (GT). The nanodrug demonstrated a higher affinity and synergistic cytotoxicity for lung carcinoma A549 cells, whilst sparing non-disease CHO cells [104].

$\text{H}_2\text{O}_2$  responsive nature of nanoceria has been exploited for tumour-selective drug delivery (Fig. 4). Controlled release of drugs (IR780 and Metformin) loaded on mesoporous silica NPs (MSN) reservoirs was achieved by employing  $\text{CeO}_2$  (~4 nm) NPs as gatekeepers sealing the channels (~2 nm pore size).  $\text{CeO}_2$  slowly etched with excessive  $\text{H}_2\text{O}_2$  in TME, eventually detaching from the pores and releasing the loaded drugs into tumour sites. Plasma half-life of the nanoplatform was ~22.5 h with almost double amount of IR780 accumulated in tumour tissues, which was a striking improvement from the ~10.8 h half-life of free IR780 [32]. Singh reported the use of amine functionalised nanoceria to cap the pores of mesoporous silica loaded with the chemotherapeutic agent doxorubicin. The nanoplatform demonstrated a typical drug release profile in an acidic medium (release %  $\text{pH} 4 > \text{pH} 5 > \text{pH} 6$ ) as the  $\text{NH}_2$ -nanoceria was protonated and detached from the mesoporous silica; on the other hand, DOX release was negligible in a neutral medium ( $\text{pH} 7.4$ ) preventing premature release of drugs under physiological conditions [123]. Sedighi developed an amine functionalised MSNs capped with nanoceria for controlled delivery of tyrosine kinase inhibitors (TKIs) sorafenib (SFN) or sunitinib (SUN) for the treatment of HCC. The nanoceria capping of MSNs potentially decreased protein adsorption that improved the colloidal stability of NPs under physiological conditions. The redox-sensitive nanoceria etched from the nanocomposite under exposure to GSH that is elevated in tumour cells to release loaded anti-cancer agents [124].

Whilst an increasing number of studies had proposed the use of nanoceria as a drug delivery agent also harbouring anti-cancer activities, Fu reported that the SOD and CAT-like activities of nanoceria are only significant at concentrations higher than  $10 \mu\text{g}/\text{mL}$  [54]. Thus, future studies must ensure that the formulations are carefully tuned whereby nanoceria and loaded drugs are delivered at doses with the highest efficacies and minimal toxicities. Researchers should also clarify the concentrations of each component in the proposed materials instead of only reporting the loaded drug or concentration of whole nanoparticles, this could help with characterising the effects of different modifications on the nanozymes.



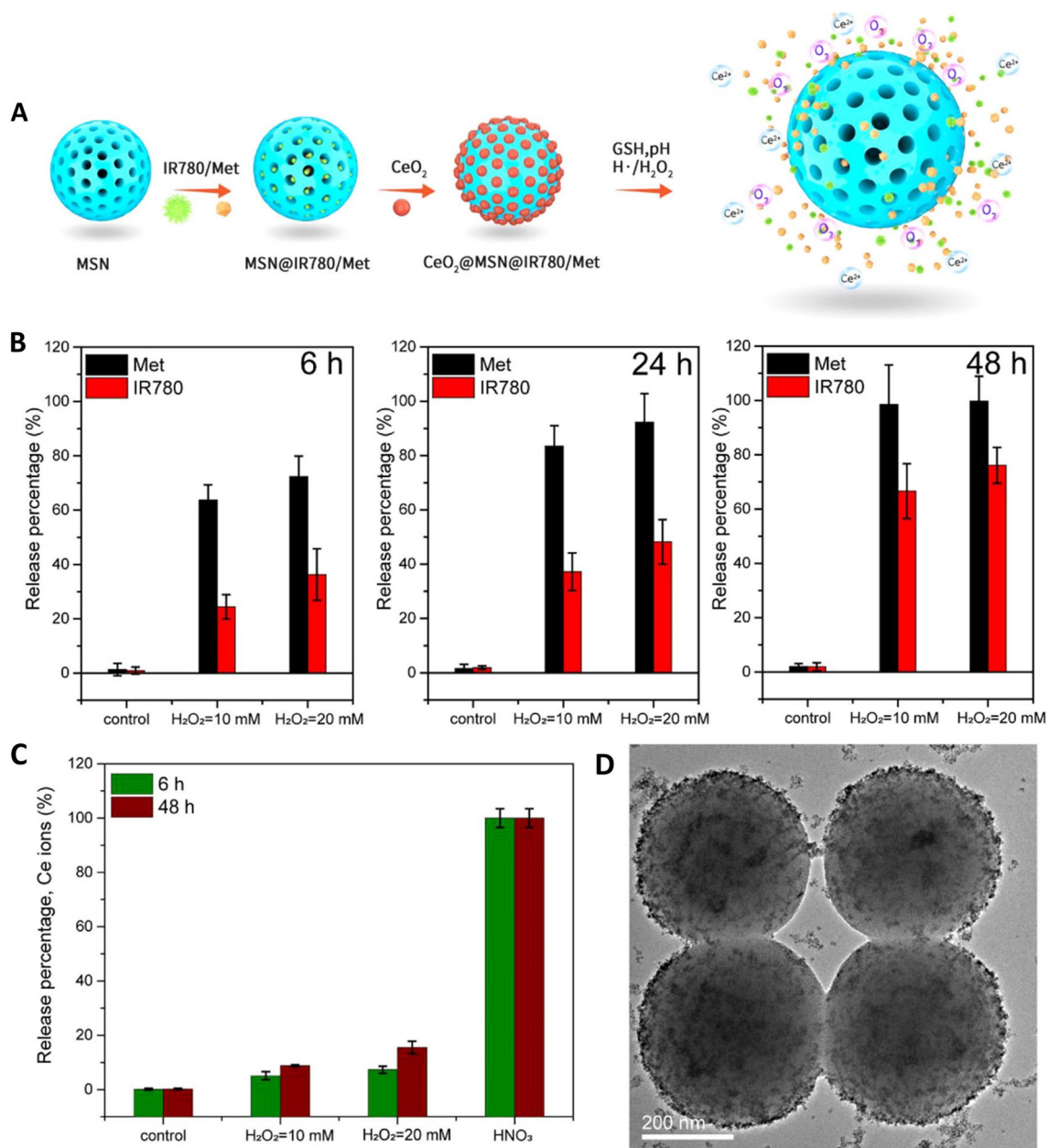


**Fig. 4**  $\text{H}_2\text{O}_2$  responsive nature of nanoceria exploited for tumour-selected drug delivery. **a** Working principle of  $\text{CeO}_2$ @MSNs@IR780/Met NPs that were synthesized by loading photosensitizer IR780 and mitochondrial respiration inhibitor Metformin into mesoporous silica nanoparticles MSNs with  $\text{CeO}_2$  as the gatekeepers. IR780 and Met were released, while  $\text{O}_2$  and  $\text{Ce}^{2+}$  were generated after the etching of  $\text{CeO}_2$  NPs in response to the special tumour microenvironment with lower pH and excessive  $\text{H}_2\text{O}_2$ . **b**, **c** In vitro release behaviour detection: **b** Time-dependant release per-

formance of IR780 (red column) and Met (black column) from the  $\text{CeO}_2$ @MSNs@IR780/Met NPs in the absence and presence of 1.0 and 2.0 M  $\text{H}_2\text{O}_2$ . **c** Etching performance of Ce NPs. Ce ions detected by inductively coupled plasma (ICP) analysis under various conditions: control, 10–20 mM  $\text{H}_2\text{O}_2$ , and nitric acid. **d** TEM image of the  $\text{CeO}_2$ @MSNs@IR780/Me nanocomposition in 20 mM  $\text{H}_2\text{O}_2$  solution after 6 h. Reprinted with permission from [32]. Copyright 2020 American Chemical Society

## Protection against treatment-induced cellular damage

The sustained release of radical species from radiation therapy leads to genetic damage and disrupts bone repair and

regeneration, resulting in bone loss and susceptibility to bone fracture in cancer patients exposed to ionising radiation [125, 126]. Wei et al. reported a  $\text{Ce}^{3+}$  dominating nanoceria (60%  $\text{Ce}^{3+}$  on the surface of nanoceria) as a potential multifaceted regulator to protect human bone marrow-derived stem cells

from ionising radiation-induced cell damage. Pre-treating cells with nanoceria significantly reduced irradiation-induced ROS generation, attenuated nuclei leakage and DNA fragmentation. Elevated expression of tumour suppressor gene p53, osteopontin, osteocalcin and bone morphogenetic protein 2; increased number of autophagic vacuole and reduced unwanted cell senescence were observed. Replenishment of NPs to the stem cells post irradiation helped to achieve optimum osteogenic differentiation [126]. Kadivar investigated the potential radio-protection and radio mitigating effect of nanoceria purchased from US Research Nanomaterials, Inc. (10–30 nm) in rats' lungs exposed to 18 Gy whole-thorax X-ray. Nanoceria administered before or after radiation treatment both demonstrated improvements in the radiation-induced histopathological changes in lung tissues [127].

Chemotherapy involving repeated systemic administration of aggressive anti-cancer drugs is associated with detrimental effects on the survival and growth of healthy cells [128–135]. For this reason, nanoceria-based materials have been engineered to protect or relieve normal tissues from the anti-cancer agents-induced toxicity. A doxorubicin (DOX) loaded, Cu-doped nanoceria enhanced the targeted tumour suppression effect of DOX whilst protecting normal cells from DOX-induced oxidative stress through its antioxidant capacity [59]. The hepatic and kidney functions and heart damage indicators of the treated groups were all in the normal range indicating excellent biosafety of this DOX-loaded nanoceria [59]. Nanoceria as a promising antioxidant and anti-inflammatory agent is also used to ameliorate chemotherapeutic agent cisplatin-induced nephrotoxicity. Swiss mice pre-treated with 2 mg/kg nanoceria (287.6 nm hydrodynamic diameter) prior to cisplatin induction showed significant improvement in general health evident by the restored body and kidney weight [136]. Reduction in levels of renal injury markers (creatinine and blood urea nitrogen), oxidative stress marker malondialdehyde and pro-inflammatory cytokines were reported [136]. Renal injury including tubular dilation and lesions found in cisplatin control groups were absent in nanoceria-treated groups [136]. All parameters and biomarkers assessed in animals that received daily injections of nanoceria for the whole duration of the experiment, were consistent with healthy control groups (isotonic saline injections), indicating the biocompatibility and safety of nanoceria [136].

These promising results further established nanoceria as an innovative treatment approach as there are higher risks of noncancer-caused deaths in diagnosed cancer patients contributed by treatment complications and infections [137]. Thus, nanomaterials with the capability of treating cancers, inhibiting metastatic progression, exerting protective effects on healthy tissues, and relieving adverse events of conventional therapies could improve patient prognosis and quality of life upon administration of treatment.

## Effects on healthy cells and normal tissues

Nanoceria-based therapeutic agents have been shown to selectively deplete or generate cytotoxic ROS depending on the pH of the microenvironment. Acidic cancerous tissues were killed but normal tissues at neutral pH were spared as nanoceria acted as ROS scavenger, producing non-toxic H<sub>2</sub>O and O<sub>2</sub> [68]. Tian et al. reported that the oxidative activity of porous CeO<sub>2</sub> nanorods and sodium polystyrene sulfonate (PN–CeO<sub>2</sub>–PSS) was inert in neutral media, hence little to no interference on healthy tissues was observed [66]. The enzymatic properties of nanoceria are also redox-sensitive that can be engineered to selectively catalyse reactions in cancerous tissues. A ceria nanozyme (ATP-HCNPs@Ce6) was reported to be an efficient PDT agent only under the presence of high-level H<sub>2</sub>O<sub>2</sub> which is characteristic of cancer cells, whilst demonstrating a protective effect on normal cells [117]. Localisation studies revealed that a dextran-coated gadolinium-doped nanoceria Ce<sub>0.9</sub>Gd<sub>0.1</sub>O<sub>1.95</sub> did not penetrate cell nuclei and comet assay confirmed that the NPs did not exhibit genotoxic effects in either normal or cancer cells [69].

As it is widely known that nanoceria favours ROS production under acidic conditions, normal cells might be damaged if nanoceria is internalised and localised in highly acidic lysosomes (pH 4.5–5.0) [138]. Upon cell internalisation, a nanoceria encapsulated in a metal–organic framework core–shell nanohybrid was found to be localised in acidic lysosomes in HeLa cells and HaCaT cells [67]. Thus, it is crucial that all nanoceria-based NPs are engineered with targeting and/or protecting moieties to minimise accidental uptake by normal cells [68]. Cancer cell membrane (CCM) was utilised to camouflage the nanoparticles for homotypic binding towards cancer cells and as a carrier to prevent premature drug leakage that might produce side effects in normal tissues [49, 68]. Enhanced uptake of CCM-coated nanoparticles by its source cancer cells [59] and excellent tumour growth suppression (cancer inhibition ratio 92.8%) with the weight of mice remained stable across the two weeks period [68] were reported. Ex vivo studies showed that a large amount of non-coated NPs deposited in the kidney and liver, while CCM-coated NPs accumulated in tumour [110]. Conjugation of ligands targeting cancer biomarkers onto nanoceria is also widely used to enhance cancer cell uptake and to mitigate accidental uptake of the nanomedicine by normal cells. Modifications of nanoceria with HA [79, 85] and FA [67] targeting CD44 receptor and folate receptor respectively that are known to be overexpressed in cancerous cells were reported. Babu Varukattu performed a competition assay by pre-treating triple-negative breast cancer cells with free HA before treatment with HA-conjugated nanoceria (HA-CePEI-NPs) and showed a significant reduction in

NPs uptake, indicating that the NPs were internalised via receptor-mediated endocytosis [85]. However, the incorporation of targeting moieties would potentially affect the therapeutic efficacy of nanoceria as the concentration of surface oxygen vacancies would be compromised. Thus, Ma et al. demonstrated targeted killing of tumour cells by engineering nanoceria of various morphologies and surface oxygen vacancies (nanoceria-rod, nanoceria-poly and nanoceria-cube) through altering ratios of sodium hydroxide and temperature of the hydrothermal reaction utilised to prepare the material. Nanoceria-rod with the highest oxygen vacancies among the three synthesised nanoceria was characterised to have an isoelectric point (IEP) of 6.2 that remained positively charged in the acidic TME ( $\text{IEP} > \text{pH}_{\text{tumour}}$ ) but negatively charged in the neutral environment ( $\text{IEP} < \text{pH}_{\text{normal}}$ ). Under the acidic TME, the nanoceria-rod selectively entered tumour cells and distributed in lysosomes and phagosomes to produce ROS and induce cell apoptosis. In contrast, the small amount of nanoceria that entered normal cells stayed in the cytoplasm with no cytotoxicity effects reported [51].

In terms of hemocompatibility, no haemolytic activity was detected in red blood cells treated with dextran-coated nanoceria  $\text{Ce}_{0.9}\text{Gd}_{0.1}\text{O}_{1.95}$  revealing potential for intravenous administration [69]. It is worthy to note that the hemocompatibility of nanoceria requires individual assessments as it varies with the characteristics and surface functionalisation of the nanoparticles [139]. Bare Cu-doped nanoceria showed slight haemolysis (4.09%) at 1000  $\mu\text{g}/\text{mL}$  but the haemolysis ratio decreased to 1.62% when coated with a cancer cell membrane [59]. No significant haemolysis was observed in red blood cells collected from healthy mice and exposed to 1  $\text{mg}/\text{mL}$  nanorod nanoceria [66].

Different methodologies were reported suggesting that nanoceria exerts no acute toxicity in animal models during treatment. H&E staining results indicated no significant morphological changes in tissues of major organs including heart, liver, spleen, lung, and kidney harvested from animals administered with nanoceria-based treatment [32, 66, 68]. Blood routine examinations including levels of red blood cells, hemoglobin, platelets, and white blood cell count were all in the normal reference ranges [59, 66, 112]. The particles at nano-scaled size were mainly non-specifically distributed in the liver, kidney, and spleen [44, 66, 68, 140] thus effects towards hepatic and renal function need to be critically assessed. Liver function biomarkers examined from the blood of treated animals including total, protein, total bilirubin, albumin, alanine aminotransferase, aspartate aminotransferase and alkaline phosphatase were reported to be in the normal ranges [32, 59, 66, 81, 112]. No significant differences in kidney function parameters including blood urea nitrogen, creatinine, glucose levels were reported comparing nanoceria-treated animals to the control group [59, 66, 112]. Cerium was also detected in the urine of treated mice,

suggesting that nanoceria can be metabolised and removed from the body through a normal excretory system [66].

It is worthy to note that the majority of research outputs reported no significant toxicities that were based on in vitro cell viability assays and in vivo adverse events that, in fact, are not capable of reproducing the tumour microenvironment [141]. In contrast to the reported excellent biocompatibility of nanoceria designed to exert cancer-killing effects, nanoceria exposure has been found to potentially induce health complications. Ballesteros reported that nanoceria demonstrated carcinogenicity in human bronchial epithelial cells BEAS-2, with tumoral effects enhanced when combined with cigarette-smoke condensate exposure [142]. The proportion of cells exhibiting cancer stem cells-like features and expression of microRNAs related to carcinogenic process were increased upon nanoceria and co-exposure treatments. Maternal exposure to nanoceria also potentially resulted in pregnancy complications [143]. Zhong et al. injected 5  $\text{mg}/\text{kg}$  nanoceria prepared with microemulsion method intravenously to pregnant BALB/c mice [144]. Whilst no damage was observed in vital organs in mother mice, fewer pups and lighter pup weights were observed compared to the control group. Uterine bleeding, severe uneven embryo development and foetal resorption rate were higher for nanoceria-treated group. Further study from the group revealed that trophoblast dysfunction mediated by excessive autophagy activation through the mTORC1 signalling pathway following nanoceria exposure led to impairment in placental development [145]. Hence, it is vital that the engineering of nanoceria platform requires the incorporation of biocompatible materials and targeting ligands to not only enhance efficacy but also to minimise potential damage to vital organs. Furthermore, the methodologies in validating biosafety of nanoceria must be thoroughly evaluated so researchers would not risk overlooking the complex biological reaction in the response of the human body to nanoparticles administration.

## Challenges in clinical translation

Despite promising findings in pre-clinical studies, there is still no nanoceria study registered on the clinical trials database (<https://www.clinicaltrials.gov>) for applications in human diseases. The limited progression towards clinical translation could be due to the drawbacks in conventional methods and the absence of standardised protocols to comprehensively characterise the surface properties, catalytic activities, and biosafety of nanoceria [146–148]. Liu and group had worked on demonstrating the use of radar analysis to assess the enzyme-mimicking activities of nanoceria prepared with varying synthesis parameters to guide the rational development and selection of a desired nanozyme [149].

However, the group only assessed differences in synthesising temperature that a lot more work would be required before a general consensus could be met. Furthermore, research laboratories generally reported characterisation of the established nanomaterial whereby the bioactive properties could not be precisely pinpointed to nanoceria itself, it could potentially be contributed by other active components or as a result of synergistic effects. Characterising nanoceria-based materials without functionalisation is not always possible due to the stability and solubility of bare cerium oxide in aqueous solutions [150]. As the correlation between surface characteristics and bioactive properties of nanoceria could not be effectively established, it becomes challenging in developing novel strategies to design and tune nanoceria-based platform to achieve desired therapeutic effects. There are lacking of studies on the interactions between nanoceria and endogenous biomolecules in physiological-relevant disease models. This resulted in the sustainability and specificity of nanoceria's ROS modulating activities in the biological systems in comparison to its natural enzymes counterparts remains unclear [87, 151]. This poses multiple challenges in accelerating bench-to-bedside as there are no established guidelines available to identify nanoceria formulation that would be effective against specific diseases and no biomarkers to stratify patient groups that would benefit from nanoceria treatment.

Discrepancies in the toxicity assessments reported also raised concerns over the safe use of nanoceria. It has been demonstrated that nanoceria does not exert genotoxicity [69, 152] but Arslan and Akbaba reported that cerium oxide in both micro and nano sizes was genotoxic on human lymphocyte cells even at low concentration (0.78 ppm) [147]. Furthermore, due to difficulties in accessing high-performance imaging modalities for pH measurement in disease models [153, 154], findings of nanoceria exerting pH-responsive catalytic effects *in vivo* are indirectly inferred from other methodologies such as  $pO_2$  level and hypoxia signals. Increased level of molecular oxygen, decreased level of hypoxic signals and enhanced efficacies of PDT were exploited to infer that nanoceria catalysed accumulation of  $O_2$ , relieving tumour hypoxia at disease sites.

Apart from that, the biocompatibility and toxicity studies of nanoceria are generally short-term effects examined in cell lines and mouse models lacking tumour heterogeneity which is a hallmark of human tumour progression and impacts clinical outcomes [155]. García-Salvador et al. revealed minor toxicity in cultured cells after acute exposures (24-h treatment) of nanoceria with a hydrodynamic size of 44.13 nm and surface charge of +36.16 mV synthesised by the conventional gel-sol process. However cytotoxic and inflammatory responses were observed in the more physiologically relevant human airway epithelial model after subchronic exposure up to 90 days [156]. Tentschert and

group performed a 2-year study on the low-dose 28.4 nm nanoceria exposure via inhalation in Wistar rats and demonstrated exposure dose and time-dependent  $CeO_2$  burden on lung and lymph nodes in close proximity of the lung [157]. Lee et al. on the other hand reported no general systemic toxicity to Sprague–Dawley rats and no reproductive and developmental toxicity to their pups after repeated oral exposure to nanoceria following testing guideline from the Organization for Economic Co-operation and Development (OECD) Working Party on Manufactured Nanomaterials [158].

The contradictions in safety assessments are likely resulting from the large variety of possible modifications during the preparation of nanoceria particles. The toxicity profile of nanoceria is therefore yet to be fully attributed. In addition to concerns over toxicology, the therapeutic potential of nanoceria in metastatic disease which is the leading cause of poor prognosis is also insufficiently studied. The reported *in vivo* anti-metastatic effects of nanoceria are deduced from the number and size of metastatic nodules forming from primary tumours at specific timepoints. There are unmet needs in investigating the therapeutic effects on the already developed metastases, long-term disease progression and survival. Thus, to accelerate the clinical translation of nanoceria, researchers should validate the safety of potential nanomedicine candidates in humans and justify that the therapeutic benefits would outweigh the possible adverse effects.

## Conclusions and future perspectives

Nanoceria-based therapeutics in pre-clinical studies focused on resolving tumour hypoxia, which is the hallmark of TME positively correlated with poor prognosis. Overconsumption of  $O_2$  by the rapid proliferation of tumour cells leads to chemotherapy tolerance and insensitivity of PDT and RT. Advantaging from the excessive  $H_2O_2$  produced by tumour cells,  $CeO_2$  NPs generate continuous supply of oxygen at the tumour site, resolving the hypoxic TME for effective therapies. The regenerative valency states, enzyme-like activities, and redox-modulatory capabilities of nanoceria presents it as a therapeutic candidate targeting the aberrant redox status in tumorous tissues. Since the valency states are self-regeneratable, treatment can potentially be given at lower or less frequent doses. The pH-responsive, dual-catalytic nature of nanoceria also protects normal tissues from oxidative stress and treatment-induced cellular damage. Interestingly, there is no comprehensive study on the correlation of  $Ce^{3+}/Ce^{4+}$  ratio and the anti-cancer effects of nanoceria *in vitro* and *in vivo*. Also, many reported studies did not include this vital parameter which makes comparison between studies complicated. Henceforth, further investigations must be performed in the future to completely elucidate the effect of

$Ce^{3+}/Ce^{4+}$  ratio on the therapeutic efficacy and toxicity of cerium-based NPs. The exact redox pathways and mechanisms affected by nanoceria in biological systems are also yet to be fully elucidated as research has been focused on the preclinical therapeutic efficacy but often lacks metabolic activities, pharmacokinetics and pharmacodynamics of the nanomaterials. The non-redox bioactivity of nanoceria has also been suggested proposing nanoceria's anticancer effects are contributed by additional non-redox mechanisms [48]. Future research should comprehensively characterise synthesised nanoceria to establish the redox and non-redox physicochemical properties of the NPs under physiological conditions and disease-specific circumstances. Metabolic fate and long-term effects of nanoceria in biological systems need to be fully assessed to ensure efficacy and safety for clinical applications. Whilst the majority of the published in vivo studies displayed therapeutic efficacy in subcutaneous tumour models, this does not reflect the true manifestation and complexity of cancer in patients. Nonetheless, this is the case in not only nanoceria-based NPs but in many preclinical anti-cancer studies whereby subcutaneous tumours are the model of choice. Hence, care must also be taken when developing animal models and investigating the potential therapeutic effects of nanoceria. The disease models should be developed to be able to represent the complexity and heterogenic nature of cancers so that studies are more clinically relevant. With thorough verification of the therapeutic effects, drug delivery efficacy, biological fate and biosafety, nanoceria-based system could serve as a promising approach to managing cancers and other ROS-related diseases. The nanomaterials that are carefully engineered with excellent biocompatibility can potentially bypass undesirable effects that arise with conventional treatments and improve clinical outcomes and quality of life for cancer patients.

**Author contributions** JT wrote the manuscript. SSM and HHT supervised the work and revised the manuscript.

**Funding** Open Access funding enabled and organized by CAUL and its Member Institutions. The authors acknowledge the support from National Health and Medical Research Council (HTT: APP1037310, APP1182347, APP2002827), and Heart Foundation (HTT: 102761).

**Availability of data and material** Not applicable.

## Declarations

**Competing interests** The authors have declared that there is no competing interest.

**Ethics approval and consent to participate** Not applicable.

**Consent for publication** All authors agree to submit the manuscript for publications.

**Open Access** This article is licensed under a Creative Commons Attribution 4.0 International License, which permits use, sharing, adaptation, distribution and reproduction in any medium or format, as long as you give appropriate credit to the original author(s) and the source, provide a link to the Creative Commons licence, and indicate if changes were made. The images or other third party material in this article are included in the article's Creative Commons licence, unless indicated otherwise in a credit line to the material. If material is not included in the article's Creative Commons licence and your intended use is not permitted by statutory regulation or exceeds the permitted use, you will need to obtain permission directly from the copyright holder. To view a copy of this licence, visit <http://creativecommons.org/licenses/by/4.0/>.

## References

1. Cancer, World Health Organization, 2022. <https://www.who.int/news-room/fact-sheets/detail/cancer>; reported 3 February 2022
2. Sung H, Ferlay J, Siegel RL, Laversanne M, Soerjomataram I, Jemal A, Bray F (2021) Global cancer statistics 2020: GLOBOCAN estimates of incidence and mortality worldwide for 36 cancers in 185 countries. *CA Cancer J Clinicians* 71(3):209–249
3. Patt D, Gordan L, Diaz M, Okon T, Grady L, Harmison M, Markward N, Sullivan M, Peng J, Zhou A (2020) Impact of COVID-19 on cancer care: how the pandemic is delaying cancer diagnosis and treatment for American seniors. *JCO Clin Cancer Inform* 4:1059–1071
4. Gurney JK, Millar E, Dunn A, Pirie R, Mako M, Manderson J, Hardie C, Jackson CGCA, North R, Ruka M, Scott N, Sarfati D (2021) The impact of the COVID-19 pandemic on cancer diagnosis and service access in New Zealand—a country pursuing COVID-19 elimination. *Lancet Reg Health West Pac* 10:100127
5. Wang X, Zhang H, Chen X (2019) Drug resistance and combating drug resistance in cancer. *Cancer Drug Resist* 2(2):141–160
6. Steeg PS (2006) Tumor metastasis: mechanistic insights and clinical challenges. *Nat Med* 12(8):895–904
7. Yang B, Chen Y, Shi J (2019) Reactive oxygen species (ROS)-based nanomedicine. *Chem Rev* 119(8):4881–4985
8. Nathan C, Cunningham-Bussell A (2013) Beyond oxidative stress: an immunologist's guide to reactive oxygen species. *Nat Rev Immunol* 13(5):349–361
9. Sena LA, Chandel NS (2012) Physiological roles of mitochondrial reactive oxygen species. *Mol Cell* 48(2):158–167
10. Szatrowski TP, Nathan CF (1991) Production of large amounts of hydrogen peroxide by human tumor cells. *Can Res* 51(3):794
11. Reczek CR, Chandel NS (2017) The two faces of reactive oxygen species in cancer. *Annu Rev Cancer Biol* 1(1):79–98
12. Aplak E, von Montfort C, Haasler L, Stucki D, Steckel B, Reichert AS, Stahl W, Brenneisen P (2020) CNP mediated selective toxicity on melanoma cells is accompanied by mitochondrial dysfunction. *PLoS ONE* 15(1):e0227926
13. Perillo B, Di Donato M, Pezone A, Di Zazzo E, Giovannelli P, Galasso G, Castoria G, Migliaccio A (2020) ROS in cancer therapy: the bright side of the moon. *Exp Mol Med* 52(2):192–203

14. Sosa V, Moliné T, Somoza R, Paciucci R, Kondoh H, Lleonart ME (2013) Oxidative stress and cancer: an overview. *Ageing Res Rev* 12(1):376–390
15. Yang H, Villani RM, Wang H, Simpson MJ, Roberts MS, Tang M, Liang X (2018) The role of cellular reactive oxygen species in cancer chemotherapy. *J Exp Clin Cancer Res* 37(1):266–266
16. Alexandre J, Hu Y, Lu W, Pelicano H, Huang P (2007) Novel action of paclitaxel against cancer cells: bystander effect mediated by reactive oxygen species. *Can Res* 67(8):3512
17. Mizutani H, Tada-Oikawa S, Hiraku Y, Kojima M, Kawanishi S (2005) Mechanism of apoptosis induced by doxorubicin through the generation of hydrogen peroxide. *Life Sci* 76(13):1439–1453
18. Kleih M, Böpple K, Dong M, Gaißler A, Heine S, Olayioye MA, Aulitzky WE, Essmann F (2019) Direct impact of cisplatin on mitochondria induces ROS production that dictates cell fate of ovarian cancer cells. *Cell Death Dis* 10(11):851
19. Nishikawa M (2008) Reactive oxygen species in tumor metastasis. *Cancer Lett* 266(1):53–59
20. Piskounova E, Agathocleous M, Murphy MM, Hu Z, Huddleston SE, Zhao Z, Leitch AM, Johnson TM, DeBerardinis RJ, Morrison SJ (2015) Oxidative stress inhibits distant metastasis by human melanoma cells. *Nature* 527(7577):186–191
21. Navya PN, Daima HK (2016) Rational engineering of physico-chemical properties of nanomaterials for biomedical applications with nanotoxicological perspectives. *Nano Converg* 3(1):1
22. Doria G, Conde J, Veigas B, Giestas L, Almeida C, Assunção M, Rosa J, Baptista PV (2012) Noble metal nanoparticles for biosensing applications. *Sensors* 12(2):1657–1687
23. Zhang Y, Li M, Gao X, Chen Y, Liu T (2019) Nanotechnology in cancer diagnosis: progress, challenges and opportunities. *J Hematol Oncol* 12(1):137
24. Alshehri S, Imam SS, Rizwanullah M, Akhter S, Mahdi W, Kazi M, Ahmad J (2021) Progress of cancer nanotechnology as diagnostics, therapeutics, and theranostics nanomedicine: preclinical promise and translational challenges. *Pharmaceutics* 13(1):24
25. Silva CO, Pinho JO, Lopes JM, Almeida AJ, Gaspar MM, Reis C (2019) Current trends in cancer nanotheranostics: metallic, polymeric, and lipid-based systems. *Pharmaceutics* 11(1):22
26. Navya PN, Kaphle A, Srinivas SP, Bhargava SK, Rotello VM, Daima HK (2019) Current trends and challenges in cancer management and therapy using designer nanomaterials. *Nano Converg* 6(1):23
27. Ruman U, Fakurazi S, Masarudin MJ, Hussein MZ (2020) Nano-carrier-based therapeutics and theranostics drug delivery systems for next generation of liver cancer nanodrug modalities. *Int J Nanomed* 15:1437–1456
28. Bhaw-Luximon A, Goonoo N, Jhurry D (2016) Chapter 6—nanotherapeutics promises for colorectal cancer and pancreatic ductal adenocarcinoma. In: Grumezescu AM (ed) *Nanobiomaterials in cancer therapy*. William Andrew Publishing, New York, pp 147–201
29. Huo M, Wang L, Chen Y, Shi J (2017) Tumor-selective catalytic nanomedicine by nanocatalyst delivery. *Nat Commun* 8(1):357
30. Hao Y, Chen Y, He X, Yu Y, Han R, Li Y, Yang C, Hu D, Qian Z (2020) Polymeric nanoparticles with ROS-responsive prodrug and platinum nanozyme for enhanced chemophotodynamic therapy of colon cancer. *Adv Sci* 7(20):2001853
31. Zhu X, Chen X, Huo D, Cen J, Jia Z, Liu Y, Liu J (2021) A hybrid nanozymes in situ oxygen supply synergistic photothermal/chemotherapy of cancer management. *Biomater Sci* 9(15):5330–5343
32. Zuo H, Hou Y, Yu Y, Li Z, Liu H, Liu C, He J, Miao L (2020) Circumventing myeloid-derived suppressor cell-mediated immunosuppression using an oxygen-generated and -economized nanoplatform. *ACS Appl Mater Interfaces* 12(50):55723–55736
33. Li Y, Yang J, Sun X (2021) Reactive oxygen species-based nanomaterials for cancer therapy. *Front Chem* 9:152
34. Gao Y, Chen K, Ma J-L, Gao F (2014) Cerium oxide nanoparticles in cancer. *Onco Targets Ther* 7:835–840
35. Reinhardt K, Winkler H (2000) Cerium mischmetal, cerium alloys, and cerium compounds, Ullmann's encyclopedia of industrial chemistry
36. Orea VM, Merino RI, Peña F (1994)  $Ce^{3+} \leftrightarrow Ce^{4+}$  conversion in ceria-doped zirconia single crystals induced by oxido-reduction treatments. *Solid State Ion* 72:224–231
37. Dhall A, Self W (2018) Cerium oxide nanoparticles: a brief review of their synthesis methods and biomedical applications. *Antioxidants (Basel)* 7(8):97
38. Yang Y, Mao Z, Huang W, Liu L, Li J, Li J, Wu Q (2016) Redox enzyme-mimicking activities of  $CeO_2$  nanostructures: intrinsic influence of exposed facets. *Sci Rep* 6(1):35344
39. Wu Y, Ta HT (2021) Different approaches to synthesising cerium oxide nanoparticles and their corresponding physical characteristics, and ROS scavenging and anti-inflammatory capabilities. *J Mater Chem B* 9:7291–7301
40. Yong JM, Fu L, Tang F, Yu P, Kuchel RP, Whitelock JM, Lord MS (2022) ROS-mediated anti-angiogenic activity of cerium oxide nanoparticles in melanoma cells. *ACS Biomater Sci Eng* 8:512–525
41. Skorodumova NV, Simak SI, Lundqvist BI, Abrikosov IA, Johansson B (2002) Quantum origin of the oxygen storage capability of ceria. *Phys Rev Lett* 89(16):166601
42. Wu Y, Yang Y, Zhao W, Xu ZP, Little PJ, Whittaker AK, Zhang R, Ta HT (2018) Novel iron oxide–cerium oxide core–shell nanoparticles as a potential theranostic material for ROS related inflammatory diseases. *J Mater Chem B* 6(30):4937–4951
43. Liu Y, Wu Y, Zhang R, Lam J, Ng JC, Xu ZP, Li L, Ta HT (2019) Investigating the use of layered double hydroxide nanoparticles as carriers of metal oxides for theranostics of ros-related diseases. *ACS Appl Bio Mater* 2(12):5930–5940
44. Wu Y, Cowin G, Moonshi SS, Tran HDN, Fithri NA, Whittaker AK, Zhang R, Ta HT (2021) Engineering chitosan nano-cocktail containing iron oxide and ceria: a two-in-one approach for treatment of inflammatory diseases and tracking of material delivery. *Mater Sci Eng C* 131:112477
45. Wu Y, Zhang R, Tran HD, Kurniawan ND, Moonshi SS, Whittaker AK, Ta HT (2021) Chitosan nanococktails containing both ceria and superparamagnetic iron oxide nanoparticles for reactive oxygen species-related theranostics. *ACS Appl Nano Mater* 4(4):3604–3618
46. Saifi MA, Seal S, Godugu C (2021) Nanoceria, the versatile nanoparticles: promising biomedical applications. *J Control Release* 338:164–189
47. Feng N, Liu Y, Dai X, Wang Y, Guo Q, Li Q (2022) Advanced applications of cerium oxide based nanozymes in cancer. *RSC Adv* 12(3):1486–1493
48. Corsi F, Caputo F, Traversa E, Ghiselli L (2018) Not only redox: the multifaceted activity of cerium oxide nanoparticles in cancer prevention and therapy. *Front Oncol* 8:309–309
49. Song G, Cheng N, Zhang J, Huang H, Yuan Y, He X, Luo Y, Huang K (2021) Nanoscale cerium oxide: synthesis, biocatalytic mechanism, and applications. *Catalysts* 11(9):1123
50. Chen W-F, Malacco CMDS, Mehmood R, Johnson KK, Yang J-L, Sorrell CC, Koshy P (2021) Impact of morphology and collagen-functionalization on the redox equilibria of nanoceria for cancer therapies. *Mater Sci Eng C* 120:111663
51. Ma B, Han J, Zhang K, Jiang Q, Sui Z, Zhang Z, Zhao B, Liang Z, Zhang L, Zhang Y (2022) Targeted killing of tumor cells based on isoelectric point suitable nanoceria-rod with high oxygen vacancies. *J Mater Chem B* 10(9):1410–1417

52. Chen M, Zhou X, Xiong C, Yuan T, Wang W, Zhao Y, Xue Z, Guo W, Wang Q, Wang H, Li Y, Zhou H, Wu Y (2022) Facet engineering of nanoceria for enzyme-mimetic catalysis. *ACS Appl Mater Interfaces* 14(19):21989–21995
53. Seal S, Jeyaranjan A, Neal CJ, Kumar U, Sakthivel TS, Sayle DC (2020) Engineered defects in cerium oxides: tuning chemical reactivity for biomedical, environmental, and energy applications. *Nanoscale* 12(13):6879–6899
54. Fu Y, Kolanthai E, Neal CJ, Kumar U, Zgheib C, Liechty KW, Seal S (2022) Engineered faceted cerium oxide nanoparticles for therapeutic miRNA delivery. *Nanomaterials* 12:4389
55. Yan H, Liu Z, Yang S, Yu X, Liu T, Guo Q, Li J, Wang R, Peng Q (2020) Stable and catalytically active shape-engineered cerium oxide nanorods by controlled doping of aluminum cations. *ACS Appl Mater Interfaces* 12(33):37774–37783
56. Mehmood R, Ariotti N, Yang JL, Koshy P, Sorrell CC (2018) pH-responsive morphology-controlled redox behavior and cellular uptake of nanoceria in fibrosarcoma. *ACS Biomater Sci Eng* 4(3):1064–1072
57. Korsvik C, Patil S, Seal S, Self WT (2007) Superoxide dismutase mimetic properties exhibited by vacancy engineered ceria nanoparticles. *Chem Commun* 14(10):1056–1058
58. Fan Y, Li P, Hu B, Liu T, Huang Z, Shan C, Cao J, Cheng B, Liu W, Tang Y (2019) A smart photosensitizer-cerium oxide nanoprobe for highly selective and efficient photodynamic therapy. *Inorg Chem* 58(11):7295–7302
59. Cheng F, Wang S, Zheng H, Yang S, Zhou L, Liu K, Zhang Q, Zhang H (2021) Cu-doped cerium oxide-based nanomedicine for tumor microenvironment-stimulative chemo-chemodynamic therapy with minimal side effects. *Colloids Surf B* 205:111878
60. Wang Z, Fu L, Zhu Y, Wang S, Shen G, Jin L, Liang R (2021) Chemodynamic/photothermal synergistic therapy based on Ce-doped Cu–Al layered double hydroxides. *J Mater Chem B* 9(3):710–718
61. Perez JM, Asati A, Nath S, Kaittanis C (2008) Synthesis of biocompatible dextran-coated nanoceria with pH-dependent antioxidant properties. *Small* 4(5):552–556
62. Asati A, Santra S, Kaittanis C, Nath S, Perez JM (2009) Oxidase-like activity of polymer-coated cerium oxide nanoparticles. *Angew Chem Int Ed* 48(13):2308–2312
63. Nourmohammadi E, Khoshdel-sarkarizi H, Nedaeinia R, Sadeghnia HR, Hasanzadeh L, Darroudi M, Kazemi Oskuee R (2019) Evaluation of anticancer effects of cerium oxide nanoparticles on mouse fibrosarcoma cell line. *J Cell Physiol* 234(4):4987–4996
64. Boedtker E, Pedersen SF (2020) The acidic tumor microenvironment as a driver of cancer. *Annu Rev Physiol* 82(1):103–126
65. Hao G, Xu ZP, Li L (2018) Manipulating extracellular tumour pH: an effective target for cancer therapy. *RSC Adv* 8(39):22182–22192
66. Tian Z, Liu H, Guo Z, Gou W, Liang Z, Qu Y, Han L, Liu L (2020) A pH-responsive polymer-CeO<sub>2</sub> hybrid to catalytically generate oxidative stress for tumor therapy. *Small* 16(47):2004654
67. Liu J, Ye LY, Xiong WH, Liu T, Yang H, Lei J (2021) A cerium oxide@metal–organic framework nanoenzyme as a tandem catalyst for enhanced photodynamic therapy. *Chem Commun* 57(22):2820–2823
68. Liu Z, Wan P, Yang M, Han F, Wang T, Wang Y, Li Y (2021) Cell membrane camouflaged cerium oxide nanocubes for targeting enhanced tumor-selective therapy. *J Mater Chem B* 9(46):9524–9532
69. Popov AL, Abakumov MA, Savintseva IV, Ermakov AM, Popova NR, Ivanova OS, Kolmanovich DD, Baranchikov AE, Ivanov VK (2021) Biocompatible dextran-coated gadolinium-doped cerium oxide nanoparticles as MRI contrast agents with high T1 relaxivity and selective cytotoxicity to cancer cells. *J Mater Chem B* 9(33):6586–6599
70. Szymanski CJ, Munusamy P, Mihai C, Xie Y, Hu D, Gilles MK, Tylliszczak T, Thevuthasan S, Baer DR, Orr G (2015) Shifts in oxidation states of cerium oxide nanoparticles detected inside intact hydrated cells and organelles. *Biomaterials* 62:147–154
71. (2006) Hypoxia/normoxia, encyclopedic reference of genomics and proteomics in molecular medicine, Springer, Berlin, pp 853–853
72. Emami Nejad A, Najafgholian S, Rostami A, Sistani A, Shojaeifar S, Esparvarinha M, Nedaeinia R, HaghjooyJavanmard S, Taherian M, Ahmadi M, Salehi R, Sadeghi B, Manian M (2021) The role of hypoxia in the tumor microenvironment and development of cancer stem cell: a novel approach to developing treatment. *Cancer Cell Int* 21(1):62
73. Wang X, Zhao D, Xie H, Hu Y (2021) Interplay of long non-coding RNAs and HIF-1 $\alpha$ : a new dimension to understanding hypoxia-regulated tumor growth and metastasis. *Cancer Lett* 499:49–59
74. Groth C, Hu X, Weber R, Fleming V, Altevogt P, Utikal J, Umanisky V (2019) Immunosuppression mediated by myeloid-derived suppressor cells (MDSCs) during tumour progression. *Br J Cancer* 120(1):16–25
75. Deng X, Shao Z, Zhao Y (2021) Solutions to the drawbacks of photothermal and photodynamic cancer therapy. *Adv Sci* 8(3):2002504
76. Sørensen BS, Horsman MR (2020) Tumor hypoxia: impact on radiation therapy and molecular pathways. *Front Oncol* 10:562
77. Hao J, Yu L, Lu H, Sakthivel TS, Seal S, Liu B, Zhao J (2021) Sensitization of breast cancer to hereceptin by redox active nanoparticles. *Am J Cancer Res* 11(10):4884–4899
78. Zhou X, You M, Wang F, Wang Z, Gao X, Jing C, Liu J, Guo M, Li J, Luo A, Liu H, Liu Z, Chen C (2021) Multifunctional graphdiyne-cerium oxide nanozymes facilitate microRNA delivery and attenuate tumor hypoxia for highly efficient radiotherapy of esophageal cancer. *Adv Mater* 33(24):2100556
79. Zeng L, Cheng H, Dai Y, Su Z, Wang C, Lei L, Lin D, Li X, Chen H, Fan K, Shi S (2021) In vivo regenerable cerium oxide nanozyme-loaded pH/H<sub>2</sub>O<sub>2</sub>-responsive nanovesicle for tumor-targeted photothermal and photodynamic therapies. *ACS Appl Mater Interfaces* 13(1):233–244
80. Jansson PJ, Kalinowski DS, Lane DJR, Kovacevic Z, Seebacher NA, Fouani L, Sahn S, Merlot AM, Richardson DR (2015) The renaissance of polypharmacology in the development of anti-cancer therapeutics: inhibition of the “Triad of Death” in cancer by Di-2-pyridylketone thiosemicarbazones. *Pharmacol Res* 100:255–260
81. Nourmohammadi E, Khoshdel-sarkarizi H, Nedaeinia R, Darroudi M, Kazemi Oskuee R (2020) Cerium oxide nanoparticles: a promising tool for the treatment of fibrosarcoma in-vivo. *Mater Sci Eng C* 109:110533
82. Adebayo OA, Akinloye O, Adaramoye OA (2021) Cerium oxide nanoparticles elicit antitumorigenic effect in experimental breast cancer induced by N-methyl-N-nitrosourea and benzo(a)pyrene in female Wistar rats. *J Biochem Mol Toxicol* 35(4):e22687
83. Datta A, Mishra S, Manna K, Saha KD, Mukherjee S, Roy S (2020) Pro-oxidant therapeutic activities of cerium oxide nanoparticles in colorectal carcinoma cells. *ACS Omega* 5(17):9714–9723
84. Abbas T, Dutta A (2009) p21 in cancer: intricate networks and multiple activities. *Nat Rev Cancer* 9(6):400–414

85. Babu Varukattu N, Lin W, Vivek R, Rejeeth C, Sabarathinam S, Yao Z, Zhang H (2020) Targeted and intrinsic activity of HA-functionalized PEI-nanoceria as a nano reactor in potential triple-negative breast cancer treatment. *ACS Appl Bio Mater* 3(1):186–196
86. Fernández-Varo G, Perramón M, Carvajal S, Oró D, Casals E, Boix L, Oller L, Macías-Muñoz L, Marfà S, Casals G, Morales-Ruiz M, Casado P, Cutillas PR, Bruix J, Navasa M, Fuster J, Garcia-Valdecasas JC, Pavel MC, Puentes V, Jiménez W (2020) Bespoken nanoceria: an effective treatment in experimental hepatocellular carcinoma. *Hepatology* 72(4):1267–1282
87. Ma Y, Tian Z, Zhai W, Qu Y (2022) Insights on catalytic mechanism of CeO<sub>2</sub> as multiple nanozymes. *Nano Res* 15:10328–10342
88. Hanahan D, Weinberg RA (2011) Hallmarks of cancer: the next generation. *Cell* 144(5):646–674
89. Tackling metastasis. *Nat Cancer* 3, 1–2 (2022). <https://doi.org/10.1038/s43018-021-00327-0>
90. Chaffer CL, Weinberg RA (2011) A perspective on cancer cell metastasis. *Science* 331(6024):1559–1564
91. Bielenberg DR, Zetter BR (2015) The contribution of angiogenesis to the process of metastasis. *Cancer J* 21(4):267–273
92. Giri S, Karakoti A, Graham RP, Maguire JL, Reilly CM, Seal S, Rattan R, Shridhar V (2013) Nanoceria: A rare-earth nanoparticle as a novel anti-angiogenic therapeutic agent in ovarian cancer. *PLoS ONE* 8(1):e54578
93. Xiao YF, Li JM, Wang SM, Yong X, Tang B, Jie MM, Dong H, Yang XC, Yang SM (2016) Cerium oxide nanoparticles inhibit the migration and proliferation of gastric cancer by increasing DHX15 expression. *Int J Nanomed* 11:3023–3034
94. Hu K, Babapoor-Farrokhran S, Rodrigues M, Deshpande M, Puchner B, Kashiwabuchi F, Hassan SJ, Asnaghi L, Handa JT, Merbs S, Eberhart CG, Semenza GL, Montaner S, Sodhi A (2016) Hypoxia-inducible factor 1 upregulation of both VEGF and ANGPTL4 is required to promote the angiogenic phenotype in uveal melanoma. *Oncotarget* 7(7):7816–7828
95. Mrozik KM, Blaschuk OW, Cheong CM, Zannettino ACW, Vandyke K (2018) N-cadherin in cancer metastasis, its emerging role in haematological malignancies and potential as a therapeutic target in cancer. *BMC Cancer* 18(1):939
96. Onder TT, Gupta PB, Mani SA, Yang J, Lander ES, Weinberg RA (2008) Loss of E-cadherin promotes metastasis via multiple downstream transcriptional pathways. *Can Res* 68(10):3645–3654
97. Chiu DK-C, Tse AP-W, Xu IM-J, Di Cui J, Lai RK-H, Li LL, Koh H-Y, Tsang FH-C, Wei LL, Wong C-M, Ng IO-L, Wong CC-L (2017) Hypoxia inducible factor HIF-1 promotes myeloid-derived suppressor cells accumulation through ENTPD2/CD39L1 in hepatocellular carcinoma. *Nat Commun* 8(1):517
98. Condamine T, Ramachandran I, Youn J-I, Gabilovich DI (2015) Regulation of tumor metastasis by myeloid-derived suppressor cells. *Annu Rev Med* 66(1):97–110
99. Zhu X, Gong Y, Liu Y, Yang C, Wu S, Yuan G, Guo X, Liu J, Qin X (2020) Ru@CeO<sub>2</sub> yolk shell nanozymes: oxygen supply in situ enhanced dual chemotherapy combined with photothermal therapy for orthotopic/subcutaneous colorectal cancer. *Biomaterials* 242:119923
100. Liu H-J, Wang J, Wang M, Wang Y, Shi S, Hu X, Zhang Q, Fan D, Xu P (2021) Biomimetic nanomedicine coupled with neoadjuvant chemotherapy to suppress breast cancer metastasis via tumor microenvironment remodeling. *Adv Funct Mater* 31(25):2100262
101. Ribera J, Portolés I, Córdoba-Jover B, Rodríguez-Vita J, Casals G, González-de la Presa B, Graupera M, Solsona-Vilarrasa E, García-Ruiz C, Fernández-Checa JC, Soria G, Tudela R, Esteve-Codina A, Espadas G, Sabidó E, Jiménez W, Sessa WC, Morales-Ruiz M (2021) The loss of DHX15 impairs endothelial energy metabolism, lymphatic drainage and tumor metastasis in mice. *Commun Biol* 4(1):1192
102. Sahai E, Astsaturov I, Cukierman E, DeNardo DG, Egeblad M, Evans RM, Fearon D, Gretchen FR, Hingorani SR, Hunter T, Hynes RO, Jain RK, Janowitz T, Jorgensen C, Kimmelman AC, Kolonin MG, Maki RG, Powers RS, Puré E, Ramirez DC, Scherz-Shouval R, Sherman MH, Stewart S, Tlsty TD, Tuveson DA, Watt FM, Weaver V, Weeraratna AT, Werb Z (2020) A framework for advancing our understanding of cancer-associated fibroblasts. *Nat Rev Cancer* 20(3):174–186
103. Asif PJ, Longobardi C, Hahne M, Medema JP (2021) The role of cancer-associated fibroblasts in cancer invasion and metastasis. *Cancers* 13(18):4720
104. Naz S, Banerjee T, Totsingan F, Woody K, Gross RA, Santra S (2021) Therapeutic efficacy of lactonic sophorolipids: nanoceria-assisted combination therapy of NSCLC using HDAC and Hsp90 inhibitors. *Nanotheranostics* 5(4):391–404
105. Ahmed HE, Iqbal Y, Aziz MH, Atif M, Batool Z, Hanif A, Yaqub N, Farooq WA, Ahmad S, Fatehmulla A, Ahmad H (2021) Green synthesis of CeO<sub>2</sub> nanoparticles from the *Abelmoschus esculentus* Extract: evaluation of antioxidant, anticancer, antibacterial, and wound-healing activities. *Molecules* 26(15):4659
106. Diamond I, McDonagh A, Wilson C, Granelli S, Nielsen S, Jaenicke R (1972) Photodynamic therapy of maglinant tumours. *Lancet* 300(7788):1175–1177
107. Zhang L, Zhong H, Zhang H, Ding C (2021) A multifunctional nano system based on DNA and CeO<sub>2</sub> for intracellular imaging of miRNA and enhancing photodynamic therapy. *Talanta* 221:121554
108. Liu X, Liu J, Chen S, Xie Y, Fan Q, Zhou J, Bao J, Wei T, Dai Z (2020) Dual-path modulation of hydrogen peroxide to ameliorate hypoxia for enhancing photodynamic/starvation synergistic therapy. *J Mater Chem B* 8(43):9933–9942
109. Pinto A, Pocard M (2018) Photodynamic therapy and photothermal therapy for the treatment of peritoneal metastasis: a systematic review. *Pleura Peritoneum* 3(4):20180124
110. Zhang C, Liu W-L, Bai X-F, Cheng S-X, Zhong Z-L, Zhang X-Z (2019) A hybrid nanomaterial with NIR-induced heat and associated hydroxyl radical generation for synergistic tumor therapy. *Biomaterials* 199:1–9
111. Murugan C, Murugan N, Sundramoorthy AK, Sundaramurthy A (2019) Nanoceria decorated flower-like molybdenum sulphide nanoflakes: an efficient nanozyme for tumour selective ROS generation and photo thermal therapy. *Chem Commun* 55(55):8017–8020
112. Jiang W, Zhang C, Ahmed A, Zhao Y, Deng Y, Ding Y, Cai J, Hu Y (2019) H<sub>2</sub>O<sub>2</sub>-sensitive upconversion nanocluster bomb for tri-mode imaging-guided photodynamic therapy in deep tumor tissue. *Adv Healthc Mater* 8(20):1900972
113. Zeng L, Zhao H, Zhu Y, Chen S, Zhang Y, Wei D, Sun J, Fan H (2020) A one-pot synthesis of multifunctional Bi<sub>2</sub>S<sub>3</sub> nanoparticles and the construction of core-shell Bi<sub>2</sub>S<sub>3</sub>@Ce<sub>6</sub>-CeO<sub>2</sub> nanocomposites for NIR-triggered phototherapy. *J Mater Chem B* 8(18):4093–4105
114. Chung A, Cui X, Audeh W, Giuliano A (2013) Current status of anti-human epidermal growth factor receptor 2 therapies: predicting and overcoming herceptin resistance. *Clin Breast Cancer* 13(4):223–232
115. Lee J-W, Bae S-H, Jeong J-W, Kim S-H, Kim K-W (2004) Hypoxia-inducible factor (HIF-1)  $\alpha$ : its protein stability and biological functions. *Exp Mol Med* 36(1):1–12
116. Wu G, Zhang Z, Chen X, Yu Q, Ma X, Liu L (2019) Chemosensitization effect of cerium oxide nanosheets by suppressing drug detoxification and efflux. *Ecotoxicol Environ Saf* 167:301–308



117. Zhou L, Li W, Wen Y, Fu X, Leng F, Yang J, Chen L, Yu X, Yu C, Yang Z (2021) Chem-inspired hollow ceria nanozymes with lysosome-targeting for tumor synergistic phototherapy. *J Mater Chem B* 9(10):2515–2523
118. Chou T-C (2006) Theoretical basis, experimental design, and computerized simulation of synergism and antagonism in drug combination studies. *Pharmacol Rev* 58(3):621
119. Dong S, Dong Y, Jia T, Liu S, Liu J, Yang D, He F, Gai S, Yang P, Lin J (2020) GSH-depleted nanozymes with hyperthermia-enhanced dual enzyme-mimic activities for tumor nanocatalytic therapy. *Adv Mater* 32(42):2002439
120. Chen Z, Xu L, Gao X, Wang C, Li R, Xu J, Zhang M, Panichayupakaranant P, Chen H (2020) A multifunctional CeO<sub>2</sub>@SiO<sub>2</sub>-PEG nanoparticle carrier for delivery of food derived proanthocyanidin and curcumin as effective antioxidant, neuroprotective and anticancer agent. *Food Res Int* 137:109674
121. Hosseinzadeh R, Khorsandi K, Esfahani HS, Habibi M, Hosseinzadeh G (2021) Preparation of cerium-curcumin and cerium-quercetin complexes and their LEDs irradiation assisted anticancer effects on MDA-MB-231 and A375 cancer cell lines. *Photodiagn Photodyn Ther* 34:102326
122. Zholobak NM, Shcherbakov AB, Ivanova OS, Reukov V, Baranchikov AE, Ivanov VK (2020) Nanoceria-curcumin conjugate: synthesis and selective cytotoxicity against cancer cells under oxidative stress conditions. *J Photochem Photobiol B* 209:111921
123. Singh RK, Patel KD, Mahapatra C, Parthiban SP, Kim T-H, Kim H-W (2019) Combinatory cancer therapeutics with nanoceria-capped mesoporous silica nanocarriers through pH-triggered drug release and redox activity. *ACS Appl Mater Interfaces* 11(1):288–299
124. Sedighi M, Rahimi F, Shahbazi M-A, Rezayan AH, Kettiger H, Einfalt T, Huwyler J, Witzigmann D (2020) Controlled tyrosine kinase inhibitor delivery to liver cancer cells by gate-capped mesoporous silica nanoparticles. *ACS Appl Bio Mater* 3(1):239–251
125. Mitchell MJ, Logan PM (1998) Radiation-induced changes in bone. *Radiographics* 18(5):1125–1136
126. Wei F, Neal CJ, Sakthivel TS, Seal S, Kean T, Razavi M, Coathup M (2021) Cerium oxide nanoparticles protect against irradiation-induced cellular damage while augmenting osteogenesis. *Mater Sci Eng C* 126:112145
127. Kadivar F, Haddadi G, Mosleh-Shirazi MA, Khajeh F, Tavasoli A (2020) Protection effect of cerium oxide nanoparticles against radiation-induced acute lung injuries in rats. *Rep Pract Oncol Radiother* 25(2):206–211
128. Lammers T, Hennink WE, Storm G (2008) Tumour-targeted nanomedicines: principles and practice. *Br J Cancer* 99(3):392–397
129. Zhao C-Y, Cheng R, Yang Z, Tian Z-M (2018) Nanotechnology for cancer therapy based on chemotherapy. *Molecules* 23(4):826
130. Ta H, Dunstan D, Dass C (2010) Anticancer activity and therapeutic applications of chitosan nanoparticles, CRC Press, Boca Raton, FL, United States, pp 271–284
131. Moonshi SS, Bejot R, Atcha Z, Vijayaragavan V, Bhakoo KK, Goggi JL (2013) A comparison of PET imaging agents for the assessment of therapy efficacy in a rodent model of glioma. *Am J Nucl Med Mol Imaging* 3(5):397–407
132. Ta HT, Dass CR, Dunstan DE (2008) Injectable chitosan hydrogels for localised cancer therapy. *J Control Release* 126(3):205–216
133. Ta HT, Dass CR, Larson I, Choong PF, Dunstan DE (2009) A chitosan–dipotassium orthophosphate hydrogel for the delivery of doxorubicin in the treatment of osteosarcoma. *Biomaterials* 30(21):3605–3613
134. Ta HT, Dass CR, Larson I, Choong PF, Dunstan DE (2009) A chitosan hydrogel delivery system for osteosarcoma gene therapy with pigment epithelium-derived factor combined with chemotherapy. *Biomaterials* 30(27):4815–4823
135. Ta HT, Dass CR, Choong PF, Dunstan DE (2009) Osteosarcoma treatment: state of the art. *Cancer Metastasis Rev* 28(1):247–263
136. Saifi MA, Sangomla S, Khurana A, Godugu C (2019) Protective effect of nanoceria on cisplatin-induced nephrotoxicity by amelioration of oxidative stress and pro-inflammatory mechanisms. *Biol Trace Elem Res* 189(1):145–156
137. Zaorsky NG, Churilla TM, Egleston BL, Fisher SG, Ridge JA, Horwitz EM, Meyer JE (2017) Causes of death among cancer patients. *Ann Oncol* 28(2):400–407
138. Zeng J, Shirihai OS, Grinstaff MW (2020) Modulating lysosomal pH: a molecular and nanoscale materials design perspective. *J Life Sci (Westlake Village)* 2(4):25–37
139. Tran HDN, Moonshi SS, Xu ZP, Ta HT (2022) Influence of nanoparticles on the haemostatic balance: between thrombosis and haemorrhage. *Biomater Sci* 10(1):10–50
140. Elahi B, Mirzaee M, Darroudi M, Sadri K, Kazemi Oskuee R (2019) Bio-based synthesis of nano-ceria and evaluation of its bio-distribution and biological properties. *Colloids Surf B Biointerfaces* 181:830–836
141. Metselaar JM, Lammers T (2020) Challenges in nanomedicine clinical translation. *Drug Deliv Transl Res* 10(3):721–725
142. Ballesteros S, Barguilla I, Marcos R, Hernández A (2021) Nanoceria, alone or in combination with cigarette-smoke condensate, induce transforming and epigenetic cancer-like features in vitro. *Nanomedicine* 16(4):293–305
143. Nedder M, Boland S, Devineau S, Zerrad-Saadi A, Rogozarski J, Lai-Kuen R, Baya I, Guibourdenche J, Vibert F, Chissey A, Gil S, Coumoul X, Fournier T, Ferecatu I (2020) Uptake of cerium dioxide nanoparticles and impact on viability, differentiation and functions of primary trophoblast cells from human placenta. *Nanomaterials* 10(7):1309
144. Zhong H, Geng Y, Chen J, Gao R, Yu C, Yang Z, Chen X, Mu X, Liu X, He J (2020) Maternal exposure to CeO<sub>2</sub>NPs during early pregnancy impairs pregnancy by inducing placental abnormalities. *J Hazard Mater* 389:121830
145. Chen Z, Geng Y, Gao R, Zhong H, Chen J, Mu X, Chen X, Zhang Y, Li F, He J (2022) Maternal exposure to CeO<sub>2</sub>NPs derails placental development through trophoblast dysfunction mediated by excessive autophagy activation. *J Nanobiotechnol* 20(1):131
146. Lord MS, Berret JF, Singh S, Vinu A, Karakoti AS (2021) Redox active cerium oxide nanoparticles: current status and burning issues. *Small* 17(51):2102342
147. Arslan K, Akbaba GB (2020) In vitro genotoxicity assessment and comparison of cerium (IV) oxide micro- and nanoparticles. *Toxicol Ind Health* 36(2):76–83
148. Casals E, Zeng M, Parra-Robert M, Fernández-Varo G, Morales-Ruiz M, Jiménez W, Puentes V, Casals G (2020) Cerium oxide nanoparticles: advances in biodistribution, toxicity, and preclinical exploration. *Small* 16(20):1907322
149. Liu X, Wu J, Liu Q, Lin A, Li S, Zhang Y, Wang Q, Li T, An X, Zhou Z, Yang M, Wei H (2021) Synthesis-temperature-regulated multi-enzyme-mimicking activities of ceria nanozymes. *J Mater Chem B* 9(35):7238–7245
150. Römer I, Briffa SM, Arroyo Rojas Dasilva Y, Hapiuk D, Trouillet V, Palmer RE, Valsami-Jones E (2019) Impact of particle size, oxidation state and capping agent of different cerium dioxide nanoparticles on the phosphate-induced transformations at different pH and concentration. *PLoS ONE* 14(6):e0217483
151. Tasdogan A, Ubellacker JM, Morrison SJ (2021) Redox regulation in cancer cells during metastasis. *Cancer Discov* 11(11):2682–2692

152. Kalyanaraman V, Naveen SV, Mohana N, Balaje RM, Nava-neethakrishnan KR, Brabu B, Murugan SS, Kumaravel TS (2019) Biocompatibility studies on cerium oxide nanoparticles—combined study for local effects, systemic toxicity and genotoxicity via implantation route. *Toxicology Research* 8(1):25–37
153. Zhang X, Lin Y, Gillies RJ (2010) Tumor pH and Its Measurement. *J Nucl Med* 51(8):1167
154. Anemone A, Consolino L, Arena F, Capozza M, Longo DL (2019) Imaging tumor acidosis: a survey of the available techniques for mapping in vivo tumor pH. *Cancer Metastasis Rev* 38(1):25–49
155. Tammela T, Sage J (2020) Investigating tumor heterogeneity in mouse models. *Annu Rev Cancer Biol* 4(1):99–119
156. García-Salvador A, Katsumiti A, Rojas E, Aristimuño C, Betanzos M, Martínez-Moro M, Moya SE, Goñi-de-Cerio F (2021) A complete in vitro toxicological assessment of the biological effects of cerium oxide nanoparticles: from acute toxicity to multi-dose subchronic cytotoxicity study. *Nanomaterials* 11(6):1577
157. Tentschert J, Laux P, Jungnickel H, Brunner J, Estrela-Lopis I, Merker C, Meijer J, Ernst H, Ma-Hock L, Keller J, Landsiedel R, Luch A (2020) Organ burden of inhaled nanoceria in a 2-year low-dose exposure study: dump or depot? *Nanotoxicology* 14(4):554–576
158. Lee J, Jeong J-S, Kim SY, Lee S-J, Shin Y-J, Im W-J, Kim S-H, Park K, Jeong EJ, Nam S-Y, Yu W-J (2020) Safety assessment of cerium oxide nanoparticles: combined repeated-dose toxicity with reproductive/developmental toxicity screening and biodistribution in rats. *Nanotoxicology* 14(5):696–710

**Publisher's Note** Springer Nature remains neutral with regard to jurisdictional claims in published maps and institutional affiliations.